

1 **Potential climatic influence on maximum stand carrying capacity for 15**  
2 **Mediterranean coniferous and broadleaf species**

3

4 Diego Rodríguez de Prado<sup>\*1,2</sup>, Roberto San Martín<sup>2</sup>, Felipe Bravo<sup>2</sup> and Celia Herrero de  
5 Aza<sup>1,2</sup>

6

7 <sup>1</sup> ECM Ingeniería Ambiental, S.L. C/Curtidores 17. Palencia (34003), Spain

8 <sup>2</sup> Instituto Universitario de Investigación en Gestión Forestal Sostenible (iUFOR), Universidad de  
9 Valladolid-INIA. Avda. Madrid 44, Palencia (34004), Spain.

10

11 \*Corresponding author: Tel: +34 639431495. Email address: rdprado@ecmingeneriaambiental.com

12

13 Published at Forest Ecology and Management (2020) 460:117824, available at

14 <https://doi.org/10.1016/j.foreco.2019.117824>



CC BY-NC-ND license. This license enables  
reusers to copy and distribute the material in any  
medium or format in unadapted form only, for  
noncommercial purposes only, and only so long  
as attribution is given to the creators

20

21

22 **Abstract**

23 Climate change projections for the Mediterranean basin predict a continuous  
24 increase in extreme drought and heat episodes, which will affect forest dynamics,  
25 structure and composition. Understanding how climate influences the maximum  
26 size-density relationship (MSDR) is therefore critical to designing adaptive  
27 silvicultural guidelines based on the potential stand carrying capacity of tree  
28 species. With this aim, data from the Third Spanish National Forest Inventory  
29 (3NFI) and WorldClim databases were used to analyze climate-related variations  
30 of the maximum stand carrying capacity for 15 species from the *Pinus*, *Fagus*  
31 and *Quercus* genera. First, basic MSDR were fitted using linear quantile  
32 regression and observed size-density data from monospecific 3NFI plots.  
33 Reference values for maximum stocking, expressed in terms of the Maximum  
34 Stand Density Index ( $SDI_{max}$ ), were estimated by species. Then, climate-  
35 dependent MSDR models including 35 annual and seasonal climatic variables  
36 were fitted. The best climate-dependent models, based on the Akaike Information  
37 Criteria (AIC) index, were used to determine the climatic drivers affecting MSDR,  
38 to analyze general and species-specific patterns and to quantify the impact of  
39 climate on maximum stand carrying capacity. The results showed that all the  
40 selected climate-dependent models improved the goodness of fit over the basic  
41 models. Among the climatic variables, spring and summer maximum  
42 temperatures were found to be key drivers affecting MSDR for the species  
43 studied. A common trend was also found across species, linking warmer and drier  
44 conditions to smaller  $SDI_{max}$  values. Based on projected climate scenarios, this  
45 suggests potential reductions in maximum stocking for these species. In this  
46 study, a new index was proposed, the Q index, for evaluating the impact of

47 climate on maximum stand carrying capacity. Our findings highlight the  
48 importance of using specific climatic variables to better characterize how they  
49 affect MSDR. The models presented in this study will allow us to better explain  
50 interactions between climate and MSDR while also providing more precise  
51 estimates concerning maximum stocking for different Mediterranean coniferous  
52 and broadleaf tree species.

53

54 **Keywords:**

55 *Self-thinning · Reineke · Maximum Stand Density Index · Forest management ·*  
56 *National Forest Inventory data*

57 **Highlights**

- 58 • MSDR and  $SDI_{max}$  estimations are significantly influenced by climate
- 59 • All selected climate-dependent MSDRs improved  $SDI_{max}$  estimations over  
60 the basic MSDRs
- 61 • Seasonal climatic variables better explain  $SDI_{max}$  variations than general  
62 climatic indexes
- 63 • Spring and summer climate changes are key drivers affecting the MSDR  
64 and  $SDI_{max}$
- 65 • Lower values of  $SDI_{max}$  are linked to warmer and drier conditions

66

67

68

69

70

## 71 1.INTRODUCTION

72

73 Maximum stand carrying capacity is a key variable in forest management and  
74 commonly used to develop site resources for sustainable, healthy and optimal  
75 stand growth. Reineke (1933) was the first to address this concept when he  
76 proposed the Maximum Stand Density Index ( $SDI_{max}$ ), an attribute that  
77 determines full site occupancy (Zeide, 2005). He discovered that for any given  
78 tree size (i.e. 25 cm), the physiological attributes of a species constrain the  
79 maximum number of trees that a fully stocked stand can support before natural  
80 mortality takes place. This relationship is widely recognized in forest science  
81 (Reineke, 1933; Drew and Flewelling, 1977) and ecology (Yoda et al., 1963;  
82 Fowler, 1981) as the Maximum Size-Density Relationship (MSDR). Also known  
83 as the self-thinning line, its applications encompass studies related to habitat  
84 distribution (Moore and Deiter, 1992), risk assessment due to abiotic and biotic  
85 factors (Fettig et al., 2007; Ducey et al., 2017) or the carbon sink capacity of  
86 forests (Woodall et al., 2011; Brunet-Navarro et al., 2016). Its use also extends  
87 to the development of forest management tools such as forest growth models  
88 (Makela et al., 2000; Yang and Titus, 2002), density management diagrams  
89 (Long and Shaw, 2005; Valbuena et al., 2008) and forest management plans  
90 (Jack and Long, 1996; Churchill et al., 2013). Initially, Reineke (1933) and Yoda  
91 et al. (1963) claimed that the MSDR, and therefore the maximum stand carrying  
92 capacity, might not be influenced by environmental conditions or site quality.  
93 However, recent studies show that this relationship varies with site quality (Bi,  
94 2001; Comeau et al., 2010), stand origin (Weiskittel et al., 2009), nutrient  
95 availability (Morris, 2003; Reyes-Hernandez et al., 2013) and stand age (Zeide,

96 2005). The influence of climate on MSDR deserves special attention, since it is  
97 widely accepted that climate is changing. Forest stands are already experiencing  
98 alterations in composition, structure and dynamics (IPCC, 2018). Relevant  
99 projections suggest that climate change will continue to affect site conditions,  
100 including stand carrying capacity, species distribution and niche suitability.  
101 Recent studies confirm that the size-density relationship is affected by climate,  
102 indicating an important decline in maximum stand carrying capacity associated  
103 with potential drought conditions in different areas of the Mediterranean basin  
104 (Condés et al., 2017; Aguirre et al., 2018). These studies frequently use annual  
105 climatic variables, such as the De Martonne Index (1926), to study climatic  
106 influences on MSDR. However, studies involving more precise (monthly or  
107 seasonal) climatic variables are needed to better understand this relationship.  
108 Kweon and Comeau (2017), for example, used periodic climatic variables such  
109 as degree-days above 5 °C, degree-days below 0°C or summer heat moisture  
110 index (the ratio between mean warmest month temperature and mean summer  
111 precipitation) to better characterize environmental conditions. They found that  
112 higher temperatures and longer frost-free periods could negatively affect the  
113 maximum stand carrying capacity. The effect of climate on MSDR has also been  
114 widely studied in mixed stands (Condés et al., 2013; del Río et al., 2014; Pretzsch  
115 and Biber, 2016; Andrews et al., 2018). Recent research has focused more on  
116 estimating size-density relationships for coniferous species (Brunet-Navarro et  
117 al., 2016; Aguirre et al., 2018), but less has been done in relation to broadleaf  
118 species. Future work should focus on discovering potential changes in the  
119 structure, composition and dynamics of monospecific broadleaf and mixed  
120 conifer-broadleaf stands. Species composition and functional traits have also

121 been indicated as key drivers affecting the maximum stand carrying capacity  
122 (Ducey et al., 2017; Kimsey et al., 2019). All these works highlight the importance  
123 of considering a range of environmental conditions, to better understand regional  
124 landscape patterns that can inform the estimation of maximum stocking. To that  
125 end, National Forest Inventory (NFI) data has proven a suitable database for  
126 studying climatic influences on MSDRs, as it covers a wide variety of forest types,  
127 stand structures and species distributed along a gradient of environmental  
128 conditions (Condés et al., 2017; Andrews et al., 2018; Toigo et al., 2018).  
129 Previous studies have used NFI data and diverse statistical methods to fit basic  
130 and climate-dependent MS DR models (Zhang et al., 2005; Hann, 2014). Principal  
131 component analysis (Hutchings and Budd, 1981; Weller, 1987; Bégin et al.,  
132 2001), stochastic frontier analysis (Bi et al., 2000; Bi, 2004; Charru et al., 2012)  
133 and linear quantile regression (Zhang et al., 2013; Vospernik and Sterba, 2015)  
134 are the methods most commonly used to fit the self-thinning line. The linear  
135 quantile regression method was chosen for the study presented here, as it can  
136 provide statistical analysis and estimates for fitting linear models to either the  
137 conditional median or other quantiles of the response variable, without stringent  
138 assumptions on the error distribution (Koenker and Bassett, 1978). Exploring the  
139 relationship between climate and the maximum carrying capacity of a forest stand  
140 is therefore key to understanding the dynamics that can inform sustainable use  
141 and management of the products and services it provides. Accordingly, the main  
142 objective of this work was to study the influence of climate on the maximum stand  
143 carrying capacity (expressed as  $SDI_{max}$ ) of 15 coniferous and broadleaf species  
144 in Spain (Table 1). The specific objectives of the study were: (i) to fit new basic  
145 and climate-dependent MS DR models and discover the key climatic drivers

146 influencing MSDR by species, (ii) to estimate the maximum stand carrying  
147 capacity for these species with and without climate influence, and (iii) to analyze  
148 and quantify general and species-specific trends in  $SDI_{max}$  variation for the  
149 species studied.

150

## 151 **2.MATERIAL AND METHODS**

152

### 153 *2.1. Data*

154

155 Spanish Third National Forest Inventory (3NFI) plots were used for this study.  
156 3NFI plots consist of four concentric circles with radii of 5,10,15 and 25 meters,  
157 in each of which multiple tree-level variables for all trees over 7.5, 12.5, 22.5 and  
158 42.5 cm diameter at breast height (1.3 m), respectively, were recorded from 1997  
159 to 2007 (Herrero and Bravo, 2012; Alberdi et al., 2016). Expansion factors were  
160 used to estimate stand variables from individual tree variables, such as density  
161 (N), quadratic mean diameter (Dg), basal area (G) and dominant height (Ho).  
162 3NFI plots located in monospecific stands of different coniferous and broadleaf  
163 species (Table 1) were selected. Plots were considered monospecific when the  
164 main species accounted for more than 90% of the total basal area. Low-density  
165 plots were discarded under the hypothesis that the MSDR depends on the  
166 climatic conditions following the methodology proposed by Condés et al. 2017. In  
167 addition, plots with quadratic mean diameter outside the 10-60 cm range were  
168 also dismissed to avoid including under-represented stands. Climatic data were  
169 obtained from Worldclim 2 (Fick and Hijmans, 2017). Worldclim 2 is a high-  
170 resolution global geo-database (30 arc seconds or ~ 1km at equator) of monthly

171 average data gathered from extensive climate observations and the NASA's  
172 Shuttle Radar Topography Mission (SRTM). Climatic variables of annual,  
173 seasonal and monthly temperature and precipitation records over a 30-year  
174 climate normal period (1970-2000) were included. Variables related to  
175 temperature were expressed in Kelvin degrees (K), since the logarithmic models  
176 fitted in this study do not accept negative values for independent variables. The  
177 Temperature Annual Range (TAR), expressed as the difference between the  
178 maximum and minimum annual temperature, and the De Martonne Index (M)  
179 were also calculated. The De Martonne Index (De Martonne, 1926), calculated  
180 as  $P/(T + 10)$  (where P is the total annual precipitation in mm, and T is the mean  
181 annual temperature in °C), is a climatic index commonly used to describe aridity  
182 or drought in a given area (Bielak et al., 2014; Condés et al., 2017; Aguirre et al.,  
183 2018). Potential evapotranspiration data from the Global Potential  
184 Evapotranspiration Geospatial Database (Trabucco and Zomer, 2009) were also  
185 considered in this study. Altogether, 35 climatic variables were used in this study  
186 to characterize climate annually and seasonally (Table 2). All climatic variables  
187 were derived from selected monospecific plots using GIS software and plot-  
188 specific latitude and longitude. Supplementary Tables 1 and 2 provide a complete  
189 statistical summary of the climatic variables used in this study.

190

## 191 *2.2. Data modeling*

192 Firstly, basic MSDR models (without climatic influence) were fitted using  
193 Reineke's (1933) equation (Eq.1) after natural logarithmic transformation  
194 (Eq.2), to obtain species-specific coefficients:

195

196 
$$N_{\max} = \alpha_0' \cdot Dg^{\beta_0} \quad (\text{Eq.1})$$

197 
$$\ln(N_{\max}) = \alpha_0 + \beta_0 \cdot \ln(Dg) \quad (\text{Eq.2})$$

198

199 where:  $N_{\max}$  is the maximum density (trees ha<sup>-1</sup>),  $Dg$  is the mean quadratic  
200 diameter (cm),  $\alpha_0$  is the species-specific intercept and  $\beta_0$  is the species-specific  
201 slope to be estimated.

202

203 Basic MSDR coefficients were estimated by linear quantile regression for each  
204 species, using the quantreg R package (Koenker, 2015) on R software (R Core  
205 Team, 2018). Models were fitted for the upper quantiles (95<sup>th</sup>, 97.5<sup>th</sup> and 99<sup>th</sup>)  
206 since the MSDR is a limiting boundary (Ducey and Knapp, 2010; Aguirre et al.,  
207 2018). Climate-dependent MSDR models were then fitted by species, to analyze  
208 the influence of climate on MSDR and maximum stand carrying capacity.  
209 Climate-dependent coefficients were obtained for each climatic variable using  
210 linear quantile regression, by expanding the coefficients in Eq.(2) as a function of  
211 climate:

212

213 
$$\ln(N_{\max}) = \alpha_0 + \alpha_1 \cdot \ln(\text{Clim}) + (\beta_0 + \beta_1 \cdot \text{Clim}) \cdot \ln(Dg) \quad (\text{Eq.3})$$

214

215 where:  $\text{Clim}$  is a climatic variable from Table 2 and  $\alpha_0$ ,  $\alpha_1$ ,  $\beta_0$  and  $\beta_1$  are the model  
216 parameters to be estimated.

217 As a result, 35 climate-dependent models were fitted for each species at the  
218 same quantiles as the basic MSDR models. The F-test, based on the extra sum  
219 of squares principle (Ratwosky, 1983), was used to test any statistically  
220 significant improvement (at  $\alpha=0.05$  significance level) of these models over the

221 basic models. Finally, significant climate-dependent models were arranged  
222 based on the Akaike Information Criterion (AIC) and pseudo- $R^2$  for quantile  
223 regression (Koenker and Machado, 1999), to determine the climatic variables that  
224 most affect MSDR by species.

225

226

227  
228  
229**Table 1:** Mean, standard deviation and range (minimum-maximum) of the main stand characteristics of the 3NFI plots selected to fit the MSDR models

Functional group	Species	n	Elev	N	Dg	G	Ho
<i>Conifers</i>	<i>Pinus canariensis</i>	1158	1286 ± 349 (246-2317)	359 ± 298 (20-1984)	29.49 ± 8.57 (11.84-50.00)	1.93 ± 1.34 (0.11-9.30)	15.31 ± 4.12 (4.50-30.50)
	<i>Pinus halepensis</i>	6074	641 ± 307 (0-1559)	413 ± 309 (33-2387)	20.51 ± 5.89 (10.01-49.30)	0.60 ± 0.43 (0.05-4.03)	9.13 ± 2.50 (2.50-25.50)
	<i>Pinus nigra</i>	2321	1101 ± 324 (183-2141)	768 ± 577 (81-4623)	20.42 ± 6.19 (10.17-53.73)	1.13 ± 0.86 (0.06-8.02)	11.1 ± 3.38 (4.00-27.79)
	<i>Pinus pinaster</i>	4427	776 ± 371 (4-1842)	512 ± 404 (20-2886)	25.86 ± 6.97 (10.06-49.93)	1.61 ± 1.15 (0.23-12.79)	12.99 ± 4.16 (4.89-36.88)
	<i>Pinus pinea</i>	1352	513 ± 289 (0-1144)	336 ± 330 (31-3233)	26.95 ± 8.27 (11.21-49.66)	1.06 ± 0.71 (0.26-7.48)	9.70 ± 2.67 (3.42-22.45)
	<i>Pinus radiata</i>	874	412 ± 249 (8-2013)	430 ± 261 (10-1678)	33.85 ± 8.83 (10.01-54.92)	3.75 ± 2.32 (0.04-12.3)	23.89 ± 5.76 (5.00-38.42)
	<i>Pinus sylvestris</i>	4082	1302 ± 329 (282-2428)	786 ± 545 (15-4333)	23.46 ± 6.99 (10.15-49.74)	1.85 ± 1.36 (0.01-11.45)	13.01 ± 3.95 (2.50-30.48)
	<i>Pinus uncinata</i>	385	1899 ± 196 (1337-2456)	746 ± 478 (40-2430)	23.73 ± 6.04 (13.21-45.27)	1.89 ± 1.00 (0.57-6.94)	11.56 ± 2.81 (5.60-20.70)
<i>Broadleaf</i>	<i>Fagus sylvatica</i>	1117	999 ± 283 (143-1943)	561 ± 414 (82-2544)	29.02 ± 9.40 (11.07-54.97)	28.01 ± 10.28 (4.03-64.84)	18.97 ± 5.00 (5.05-36.35)
	<i>Quercus faginea</i>	685	869 ± 221 (146-1552)	643 ± 590 (28-3088)	17.18 ± 6.54 (10.01-39.94)	0.58 ± 0.75 (0.02-5.82)	7.89 ± 2.38 (2.50-20.46)
	<i>Quercus ilex</i>	3609	661 ± 309 (57-1980)	281 ± 333 (41-2005)	23.57 ± 10.09 (10.00-49.98)	6.85 ± 3.75 (1.39-22.78)	6.18 ± 1.38 (0.95-11.75)
	<i>Quercus petraea</i>	201	1006 ± 302 (112-1622)	697 ± 565 (38-3392)	24.17 ± 8.81 (10.58-48.02)	2.13 ± 1.82 (0.40-13.35)	12.86 ± 4.07 (5.54-28.82)
	<i>Quercus pyrenaica</i>	1879	1029 ± 247 (150-1898)	751 ± 664 (33-5125)	18.91 ± 7.79 (10.01-49.85)	0.80 ± 0.97 (0.08-9.84)	10.33 ± 2.90 (2.64-22.52)
	<i>Quercus robur</i>	560	495 ± 236 (31-1598)	403 ± 316 (52-1791)	29.01 ± 9.59 (11.07-54.92)	20.42 ± 9.71 (3.75-61.49)	13.97 ± 4.11 (1.85-28.98)
	<i>Quercus suber</i>	687	398 ± 211 (18-1065)	243 ± 228 (41-1287)	31.9 ± 10.31 (12.06-54.09)	14.12 ± 6.92 (3.16-41.87)	8.13 ± 2.11 (2.38-15.55)

230  
231  
232  
233  
234

*n* - Number of monspecific plots, *Elev* - Plot altitude (m), *N* - Stand density (trees ha<sup>-1</sup>), *Dg* - Quadratic mean diameter (cm), *G* - Basal area (m<sup>2</sup> ha<sup>-1</sup>), *Ho* - Dominant height (m)

235  
236

**Table 2:** List of climatic variables used in this study

Variable	Definition	237
T	Annual Mean Temperature (Kelvin degrees)	238
T <sub>i</sub>	Mean Temperature (Kelvin) of the i Season (i = 1,2,3,4)	239
MNT	Annual mean Minimum Temperature (Kelvin degrees)	240
MNT <sub>i</sub>	Minimum Temperature (Kelvin degrees) of the i Season (i = 1,2,3,4)	241
MXT	Annual Mean Maximum Temperature (Kelvin degrees)	242
MXT <sub>i</sub>	Maximum Temperature (Kelvin degrees) of the i Season (i = 1,2,3,4)	243
MXTWM	Maximum Temperature of Warmest Month (Kelvin degrees)	244
MNTCM	Minimum Temperature of Coldest Month (Kelvin degrees)	245
TAR	Temperature Annual Range (Kelvin degrees) (MXTWM - MNTCM)	246
P	Total Annual Precipitation (mm)	247
P <sub>i</sub>	Total Precipitation (mm) of the i Season (i = 1,2,3,4)	248
PWM	Precipitation of Wettest Month (mm)	249
PDM	Precipitation of Driest Month (mm)	250
M	Annual De Martonne Index (mm °C <sup>-1</sup> )	251
M <sub>i</sub>	De Martonne Index (mm °C <sup>-1</sup> ) of the i Season (i = 1,2,3,4)	252
PET	Annual Potential Evapotranspiration (mm)	253
PET <sub>i</sub>	Potential Evapotranspiration (mm) of the i Season (i = 1,2,3,4)	254

261  
262  
263  
264

*i: 1=Autumn (October, November, December), 2=Winter (January, February, March), 3=Spring (April, May, June), 4=Summer (July, August, September)*

### 265 2.3. Climatic influence on maximum stand carrying capacity

266

267 Maximum stand carrying capacity was expressed as the Maximum Stand Density  
268 Index (SDI<sub>max</sub>), derived from Reineke's (1933) equation. Reference values for  
269 SDI<sub>max</sub> (SDI<sub>maxREF</sub>) were calculated by species, using estimated coefficients from  
270 basic MSDR models (Eq.2).

271

$$272 \quad \text{SDI}_{\text{maxREF}} = e^{[\alpha_0 + \beta_0 \cdot \ln(25)]} \quad (\text{Eq.4})$$

273

274 In a similar way, estimated coefficients from the selected climate-dependent  
275 models were used to calculate the climate-dependent SDI<sub>max</sub> by species [Eq.5]:

276

$$277 \quad \text{SDI}_{\text{max}}(\text{Clim}) = e^{[(\alpha_0 + \alpha_1 \cdot \ln(\text{Clim})) + (\beta_0 + \beta_1 \cdot \text{Clim}) \cdot \ln(25)]} \quad (\text{Eq.5})$$

278 where  $SDI_{max}(Clim)$  is the function of the maximum stand carrying capacity for  
 279 each species and climatic variable  $Clim$  and  $\alpha_0$ ,  $\alpha_1$ ,  $\beta_0$  and  $\beta_1$  are the estimated  
 280 coefficients from climate-dependent MSDR models.

281

282 To visually detect trends in  $SDI_{max}$  variation,  $SDI_{max}(Clim)$  values were obtained  
 283 and plotted along the range of values (percentiles 1 to 99) for each climatic  
 284 variable selected. Then, the Q index was proposed in order to quantify the  $SDI_{max}$   
 285 variation a species shows in a region along a range of different climatic  
 286 conditions. First, the difference between  $SDI_{max}(Clim)$  values obtained from the  
 287 climate-dependent models (Eq. 5) with respect to species-specific  $SDI_{maxREF}$   
 288 obtained from (Eq. 4) was considered (Figure 1). By integrating them between  
 289 the 1<sup>st</sup> and the 99<sup>th</sup> percentile of the climatic variable, the area between the  $SDI_{max}$   
 290 ( $Clim$ ) function and the  $y = SDI_{maxREF}$  line was then determined. This area is  
 291 known as the Surface Between Curves (SBC). To relativize the SBC to the  
 292  $SDI_{maxREF}$  reference value and make it comparable among species and climatic  
 293 drivers, the Q index was calculated as shown in Eq.6.

294  
 295  
 296  
 297  
 298  
 299  
 300  
 301  
 302  
 303  
 304  
 305  
 306  
 307  
 308

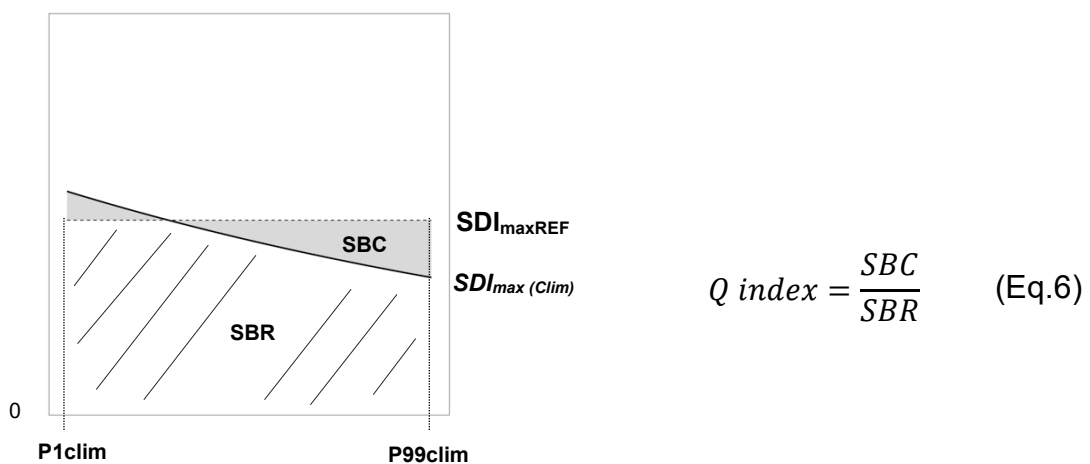


Figure 1: Graphical representation of the Q index

309 where SBR (Surface Below Reference) represents the area below the reference  
310 line  $y = SDI_{\max\text{REF}}$ , i.e.,  $SBR = SDI_{\max\text{REF}} * (P99_{\text{clim}} - P1_{\text{clim}})$  and  $P1_{\text{clim}}$  and  
311  $P99_{\text{clim}}$  are the 1<sup>st</sup> and the 99<sup>th</sup> percentile of the climatic variable.

312

313

### 314 **3.RESULTS**

#### 315 *3.1. Basic MSDR models*

316

317 The intercept ( $\alpha_0$ ) and slope ( $\beta_0$ ) of the basic MSDRs were highly significant ( $p <$   
318  $0.001$ ) for all the coniferous (Table 3) and broadleaf species (Table 4) studied.

319 Since  $SDI_{\max\text{REF}}$  estimate results were very low for the 95<sup>th</sup> and very high for the  
320 99<sup>th</sup> quantiles compared to similar studies, the 97.5<sup>th</sup> quantile was selected as the  
321 reference for each model, to allow for comparison of results among all the species

322 studied. The results of the basic MSDR models fitted at these quantiles are

323 available in Supplementary Table 3. Of the coniferous species, *Pinus pinea* (-

324 2.1855) and *Pinus pinaster* (-1.9063) presented the steepest slopes of the basic

325 MSDRs, while *Pinus sylvestris* (-1.7524) and *Pinus uncinata* (-1.7336) presented

326 the flattest slopes. Estimated  $SDI_{\max\text{REF}}$  values for the coniferous species ranged

327 from 526 (*Pinus halepensis*) to 1178 (*Pinus radiata*) trees per hectare (Table 5).

328 In general, broadleaf species presented smaller maximum stand carrying

329 capacities (from 319 to 995 trees per hectare) than coniferous species. Results

330 for these species fell along a gradient; *Quercus ilex* (-2.0951) had higher

331 intercepts and shallower slopes, followed by *Quercus suber*, *Fagus sylvatica*,

332 *Quercus pyrenaica*, *Quercus faginea*, *Quercus petraea*, and finally *Quercus robur*

333 with the least pronounced slope (-1.6698) (Table 4). Basic MSDR trajectories are  
334 shown by species in Figures 2 and 3.

335

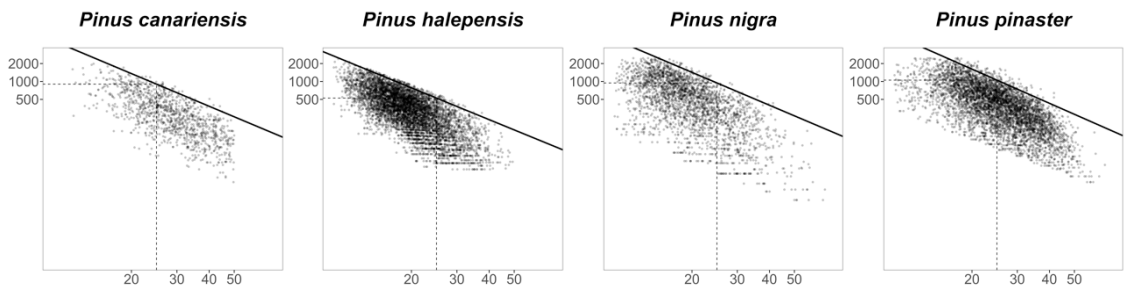
### 336 3.2. Climate-dependent MSDR models

337

338 Coefficients for the best climate-dependent MSDR models fitted at the 97.5<sup>th</sup>  
339 quantile are presented in Table 3 (coniferous species) and Table 4 (broadleaf  
340 species). A complete list of all fitted climate-dependent MSDR models is available  
341 in Supplementary Table 4. The results indicated that climatic variables related to  
342 temperature better explained the influence of climate on MSDR, for both conifers  
343 and broadleaf species. Specifically, seasonal (MXT<sub>i</sub>) and annual (MXT) maximum  
344 temperatures were the most representative climatic variables among the 35  
345 studied. Climate-dependent models including Maximum Summer Temperature  
346 (MXT<sub>4</sub>) were selected in 8 (4 conifer and 4 broadleaf) of the 15 species, followed  
347 by models including Maximum Spring Temperature (MXT<sub>3</sub>), Maximum  
348 Temperature of the Warmest Month (MXT<sub>W</sub>M) and Maximum Annual  
349 Temperature (MXT). For all species excepting, spring and summer consistently  
350 appeared as key periods, with significant interaction between climate and MSDR.  
351 Among the conifers studied, the models selected for *Pinus halepensis*, *Pinus*  
352 *nigra*, *Pinus pinaster* and *Pinus sylvestris* indicated maximum temperatures as  
353 key variables for explaining climatic influence on MSDR. In contrast, aridity,  
354 precipitation and potential evapotranspiration was the variables that most  
355 influenced MSDR for *Pinus canariensis*, *Pinus pinea*, *Pinus radiata* and *Pinus*  
356 *uncinata* (Table 3). Only three climatic models were significant for *Pinus radiata*,  
357 which may be due to a high concentration of selected monospecific plots in a

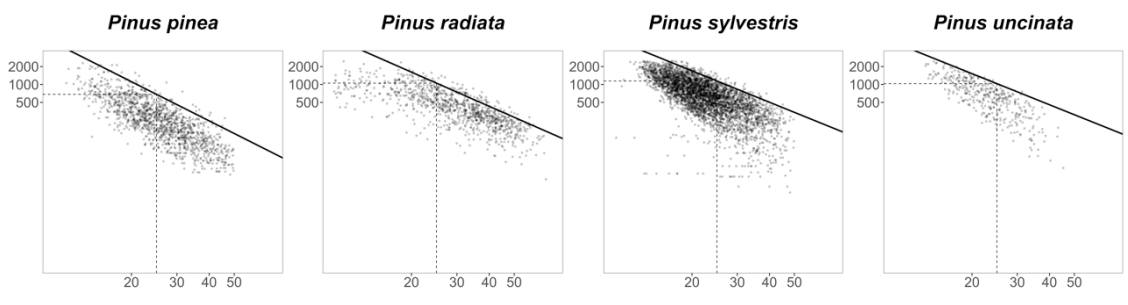
358 specific area without a wide climatic variability. Among the broadleaf species  
359 studied, temperature was also found to be a key driver affecting MSDR, since  
360 most of the climate-dependent models selected were related to these variables  
361 (Table 4). Maximum temperatures were found to be key drivers for *Quercus*  
362 *petraea* and *Quercus pyrenaica*, while *Quercus robur* was affected by minimum  
363 temperatures. The best models for *Quercus ilex* and *Quercus suber* indicated  
364 that potential evapotranspiration played an important role in explaining changes  
365 in MSDR and  $SDI_{max}$  for these species. Aridity also influenced the MSDR of  
366 *Fagus sylvatica* and *Quercus faginea* according to the best models for these  
367 species. However, the other selected models for *Quercus faginea* were related  
368 to changes in summer temperatures. For all species, selected climate-dependent  
369 MSDR significantly improved the goodness of fit, in terms of AIC and pseudo- $R^2$ ,  
370 compared to the basic models. Among the coniferous species, *Pinus pinea* and  
371 *Pinus radiata* selected models showed the highest pseudo- $R^2$  with values close  
372 to 0.40 (Table 3). *Pinus canariensis* models showed the highest AIC reduction ( $\Delta$   
373 AIC ranging -7 and -11.3%) with respect to the basic MSDR model. For *Pinus*  
374 *nigra*, *Pinus sylvestris* and *Pinus radiata*, however, inclusion of a climatic variable  
375 in the basic MSDR model did little to improve its efficiency ( $\Delta$  AIC close to -2%).  
376 Compared to conifers, broadleaf results generally presented higher pseudo- $R^2$   
377 values and greater differences in AIC with respect to the basic MSDR models  
378 (Table 4). Climate-dependent models for *Fagus sylvatica*, *Quercus ilex* and  
379 *Quercus suber* presented the highest pseudo- $R^2$  values among the 15 species.  
380  
381  
382

383



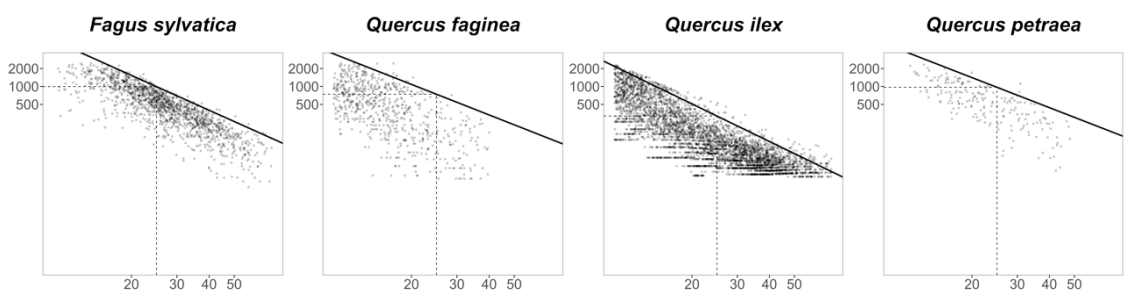
384

385



386

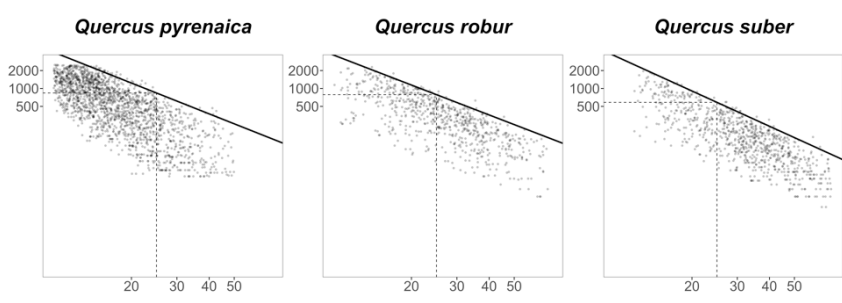
387



388

389

390



*Dg (cm)*

391

392

393

394

395

**Figure 2:** Maximum Size-Density Relationships (MSDR) for the 15 coniferous and broadleaf species studied, plotted on a log-log scale for the selected monospecific stands. Self-thinning boundary lines fitted by quantile regression (97.5<sup>th</sup> quantile) are represented by solid lines. Dashed lines represent the  $SDI_{maxREF}$  (maximum number of trees at a Dg reference of 25 cm).

396

397

398

399

400

401

402

403

404

405  
406  
407  
408

**Table 3:** Species-specific coefficients, SDI<sub>max</sub> estimates and goodness of fit in terms of Akaike's Information Criterion (AIC) and pseudo-R<sup>2</sup> coefficient for the basic and the top five climate-dependent MSDR models fitted by linear quantile regression (97.5<sup>th</sup> quantile) for coniferous species.

Species	Model	$\alpha_0$	$\alpha_1$	$\beta_0$	$\beta_1$	AIC	pseudo-R <sup>2</sup>	Q index
<i>Pinus canariensis</i>	<b>basic</b>	<b>12.672 ***</b>	-	<b>-1.8226 ***</b>	-	<b>2616.9</b>	<b>0.3378</b>	-
	P1	3.639 ***	2.448 ***	-2.0891 ***	-	2320.8	0.4178	0.305
	PWM	4.176 ***	2.059 ***	-1.9567 ***	-	2347.4	0.4111	0.251
	P	13.161 ***	-	-2.6082 ***	0.0015 ***	2364.4	0.4067	0.245
	P2	12.989 ***	-	-2.3961 ***	0.0075 ***	2420.9	0.3921	0.189
	M1	11.738 ***	1.061 ***	-1.8500 ***	-	2431.5	0.3893	0.189
<i>Pinus halepensis</i>	<b>basic</b>	<b>11.982 ***</b>	-	<b>-1.7760 ***</b>	-	<b>12622.5</b>	<b>0.3388</b>	-
	M	9.241 ***	0.886 ***	-1.5559 ***	-0.0095 **	12325.5	0.3549	0.063
	MXT3	96.948 ***	-14.977 ***	-1.7045 ***	-	12368.1	0.3526	0.079
	MXT4	105.595 ***	-16.445 ***	-1.7171 ***	-	12383.7	0.3517	0.077
	MXTWM	100.504 ***	-15.542 ***	-1.7134 ***	-	12394.4	0.3512	0.073
	PWM	8.722 ***	0.784 ***	-1.6057 ***	-0.0026 *	12401.9	0.3509	0.051
<i>Pinus nigra</i>	<b>basic</b>	<b>12.756 ***</b>	-	<b>-1.8346 ***</b>	-	<b>5117.9</b>	<b>0.2965</b>	-
	MXT3	140.953 ***	-22.536 ***	-1.9324 ***	-	5010.9	0.3128	0.123
	MXT	154.667 ***	-24.995 ***	-1.9154 ***	-	5028.5	0.3102	0.119
	MXT4	104.610 ***	-16.094 **	-1.9119 ***	-	5045.9	0.3076	0.091
	MXT2	13.019 ***	-	5.7005 ***	-0.0268 ***	5046.7	0.3075	0.119
	P2	11.821 ***	0.290 ***	-1.8973 ***	-	5047.8	0.3073	0.098
<i>Pinus pinaster</i>	<b>basic</b>	<b>13.096 ***</b>	-	<b>-1.9063 ***</b>	-	<b>10593.0</b>	<b>0.2716</b>	-
	MXT	13.446 ***	-	4.1770 ***	-0.0213 ***	10229.0	0.3011	0.129
	MXT3	13.365 ***	-	3.5759 ***	-0.0190 ***	10241.6	0.3001	0.128
	T3	13.324 ***	-	3.9110 ***	-0.0206 ***	10296.4	0.2958	0.121
	MXT4	13.462 ***	-	2.6955 ***	-0.0159 ***	10307.5	0.2949	0.114
	MXT2	13.389 ***	-	3.3318 ***	-0.0187 ***	10317.1	0.2941	0.114
<i>Pinus pinea</i>	<b>basic</b>	<b>13.562 ***</b>	-	<b>-2.1855 ***</b>	-	<b>3270.9</b>	<b>0.3887</b>	-
	P4	15.072 ***	-0.460 *	-2.4379 ***	0.0093 ***	3139.5	0.4185	0.262
	M4	13.531 ***	-0.467 **	-2.4556 ***	0.2919 ***	3144.0	0.4176	0.257
	P	13.213 ***	-	-2.2271 ***	0.0003 **	3210.7	0.4026	0.131
	TAR	77.368 **	-11.127 *	-2.2790 ***	-	3213.2	0.4020	0.143
	M	13.304 ***	-	-2.2518 ***	0.0077 *	3216.7	0.4013	0.155
<i>Pinus radiata</i>	<b>basic</b>	<b>12.947 ***</b>	-	<b>-1.8254 ***</b>	-	<b>1432.8</b>	<b>0.3723</b>	-
	PET3	110.968 ***	-21.507 ***	-8.0490 ***	0.0652 ***	1402.4	0.3845	0.058
	PET4	88.959 ***	-16.269 **	-6.5496 ***	0.0441 **	1409.2	0.3821	0.062
	PET1	6.920 **	1.675 *	-1.3894 ***	-0.0119 **	1421.2	0.3778	0.020
<i>Pinus sylvestris</i>	<b>basic</b>	<b>12.685 ***</b>	-	<b>-1.7524 ***</b>	-	<b>7718.9</b>	<b>0.368</b>	-
	TAR	66.470 ***	-9.442 ***	-1.7478 ***	-	7594.7	0.3777	0.078
	MNTCM	617.791 ***	-108.147 ***	-40.0934 ***	0.1425 ***	7630.1	0.3751	0.109
	MXTWM	74.540 ***	-10.872 ***	-1.7675 ***	-	7637.6	0.3744	0.075
	MXT4	71.686 ***	-10.376 ***	-1.7699 ***	-	7643.9	0.3739	0.073
	MXT3	58.945 ***	-8.154 ***	-1.7767 ***	-	7653.0	0.3732	0.064
<i>Pinus uncinata</i>	<b>basic</b>	<b>12.519 ***</b>	-	<b>-1.7336 ***</b>	-	<b>556.6</b>	<b>0.4414</b>	-
	PET3	12.918 ***	-	-1.6378 ***	-0.0031 **	534.6	0.4586	0.068
	PET4	16.777 ***	-0.838 ***	-1.8979 ***	-	535.5	0.4580	0.063
	PET	12.899 ***	-	-1.6288 ***	-0.0004 **	535.6	0.4578	0.108
	PET2	12.908 ***	-	-1.6784 ***	-0.0077 **	536.7	0.4571	0.062
	P2	11.386 ***	0.364 ***	-1.9112 ***	-	538.1	0.4561	0.052

409  
410  
411  
412  
413  
414  
415  
416  
417  
418  
419  
420  
421  
422  
423

\*\*\* $p < 0.001$ ; \*\* $p < 0.01$ ; \* $p < 0.05$

Note: Fewer than 5 significant climate-dependent MSDR models were found for *Pinus radiata* and *Pinus uncinata*.

424  
425  
426  
427

**Table 4:** Species-specific coefficients, SDI<sub>max</sub> estimates and goodness of fit in terms of Akaike's Information Criterion (AIC) and pseudo-R<sup>2</sup> coefficient for the basic and the best climate-dependent MSDR models fitted by linear quantile regression (97.5<sup>th</sup> quantile) for broadleaf species.

Species	Model	$\alpha_0$	$\alpha_1$	$\beta_0$	$\beta_1$	AIC	pseudo-R <sup>2</sup>	Q index
<i>Fagus sylvatica</i>	<b>basic</b>	<b>13.170 ***</b>	-	<b>-1.9471 ***</b>	-	<b>1577.1</b>	<b>0.5137</b>	-
	MXT3	12.870 ***	-	2.0880 ***	-0.0137 ***	1507.5	0.5290	0.085
	T3	12.813 ***	-	2.0872 *	-0.0138 ***	1510.2	0.5285	0.085
	MXT2	75.624 ***	-11.138 ***	-1.8360 ***	-	1512.2	0.5281	0.070
	PET1	12.911 ***	-	-1.5935 ***	-0.0085 ***	1514.5	0.5276	0.061
	M1	12.133 ***	0.671 ***	-2.0013 ***	-	1514.9	0.5275	0.135
<i>Quercus faginea</i>	<b>basic</b>	<b>12.097 ***</b>	-	<b>-1.7055 ***</b>	-	<b>2003.5</b>	<b>0.1811</b>	-
	MXTWM	247.037 ***	-41.233 ***	-1.7874 ***	-	1883.7	0.2508	0.315
	TAR	12.606 ***	-	12.9044 ***	-0.0495 ***	1886.9	0.2490	0.350
	MXT4	254.074 ***	-42.519 ***	-1.7485 ***	-	1899.6	0.2420	0.315
	T4	271.627 ***	-45.750 ***	-1.6856 ***	-	1910.6	0.2359	0.303
	M	9.667 ***	0.812 ***	-1.8657 ***	-	1915.9	0.2329	0.188
<i>Quercus ilex</i>	<b>basic</b>	<b>12.508 ***</b>	-	<b>-2.0951 ***</b>	-	<b>8099.8</b>	<b>0.5025</b>	-
	PET3	11.777 ***	-	-1.3094 ***	-0.0044 ***	7398.6	0.5487	0.211
	PET	11.773 ***	-	-1.4050 ***	-0.0004 ***	7449.7	0.5455	0.207
	MXT3	11.899 ***	-	5.0064 ***	-0.0234 ***	7474.1	0.5440	0.215
	MXTWM	11.969 ***	-	4.7651 ***	-0.0223 ***	7484.2	0.5433	0.172
	PET2	11.865 ***	-	-1.5025 ***	-0.0087 ***	7491.1	0.5429	0.159
<i>Quercus petraea</i>	<b>basic</b>	<b>12.277 ***</b>	-	<b>-1.6777 ***</b>	-	<b>431.3</b>	<b>0.3877</b>	-
	MXT	-489.861 ***	88.759 ***	36.5003 ***	-0.1334 ***	357.6	0.4954	0.242
	MXT4	12.593 ***	-	9.0312 ***	-0.0370 ***	358.5	0.4917	0.247
	MXT3	12.615 ***	-	7.5139 ***	-0.0323 ***	360.0	0.4899	0.230
	MXTWM	12.382 ***	-	8.8624 ***	-0.0360 ***	360.8	0.4889	0.227
	T4	12.674 ***	-	11.0925 ***	-0.0446 ***	361.6	0.4878	0.240
<i>Quercus pyrenaica</i>	<b>basic</b>	<b>12.271 ***</b>	-	<b>-1.7203 ***</b>	-	<b>4718.4</b>	<b>0.2962</b>	-
	T4	-187.581 *	35.255 *	17.946 ***	-0.0679 ***	4537.2	0.3300	0.213
	MNT4	12.312 ***	-	7.1163 ***	-0.0309 ***	4566.5	0.3244	0.186
	MXTWM	12.335 ***	-	5.6320 ***	-0.0250 ***	4570.0	0.3238	0.191
	MXT3	-310.973 *	57.023 *	24.1039 ***	-0.0892 ***	4577.6	0.3228	0.204
	MXT4	12.328 ***	-	5.5596 ***	-0.0248 ***	4578.1	0.3223	0.182
<i>Quercus robur</i>	<b>basic</b>	<b>12.043 ***</b>	-	<b>-1.6698 ***</b>	-	<b>1017.7</b>	<b>0.4394</b>	-
	MNT3	-795.789 ***	143.317 ***	49.1578 ***	-0.1812 ***	974.7	0.4624	0.120
	MNT	-820.659 ***	147.740 ***	51.1787 ***	-0.1885 ***	981.1	0.4594	0.125
	MNT2	-605.574 ***	109.939 ***	37.8316 ***	-0.1435 ***	985.5	0.4572	0.123
	MNT4	-1112.201 ***	198.611 ***	70.2864 ***	-0.2505 ***	989.2	0.4554	0.131
	MNT1	-624.820 **	113.08 **	39.0364 **	-0.1458 **	993.6	0.4533	0.115
<i>Quercus suber</i>	<b>basic</b>	<b>12.704 ***</b>	-	<b>-1.9674 ***</b>	-	<b>1340.2</b>	<b>0.4839</b>	-
	PET3	11.948 ***	-	-1.2349 ***	-0.0043 ***	1233.6	0.5231	0.176
	MXTWM	12.097 ***	-	9.7879 ***	-0.0385 ***	1235.9	0.5223	0.208
	PET4	11.846 ***	-	-1.3656 ***	-0.0025 ***	1239.2	0.5211	0.150
	MXT4	-670.091 **	119.608 **	43.6583 ***	-0.1515 ***	1239.5	0.5217	0.147
	MXT3	12.343 ***	-	9.4775 **	-0.0384 ***	1243.8	0.5195	0.185

428  
429  
430  
431

\*\*\* $p < 0.001$ ; \*\* $p < 0.01$ ; \* $p < 0.05$ ; ns non-significant

432

### 433 3.3. Climatic influence on maximum stand carrying capacity

434

435 In this study, climate was found to have significant influence on MSDR, and  
436 therefore on the maximum stand carrying capacity (SDI<sub>max</sub>). The best climate-

437 dependent models for each species revealed a common trend in SDI<sub>max</sub> variation  
 438 for coniferous and broadleaf species (Figure 4 and Figure 5). The results  
 439 indicated that higher SDI<sub>max</sub> values were negatively linked to temperature and  
 440 positively linked to precipitation (Table 5). Accordingly, higher maximum  
 441 temperatures led to smaller SDI<sub>max</sub> values for *Pinus nigra*, *Pinus pinaster*, *Fagus*  
 442 *sylvatica*, *Quercus faginea* and *Quercus petraea*, while increments in  
 443 precipitation led to higher SDI<sub>max</sub> values for *Pinus canariensis* and *Quercus pinea*.  
 444 A particular behaviour of SDI<sub>max</sub> variation was found for *Pinus pinea* and *Pinus*  
 445 *radiata*, with a *SDI<sub>max</sub> (Clim)* distribution presenting a parabolic shape with a  
 446 minimum reached close to the median of the P4 (*Pinus pinea*) and PET3 (*Pinus*  
 447 *radiata*) range.

448

449 **Table 5:** SDI<sub>max</sub> estimates for the different percentiles of the selected climate variable (best climate-  
 450 dependent model) and Q index for the species studied.

451  
452

Functional Group	Species	Clim	SDI <sub>max</sub> REF	SDI <sub>max</sub> (Clim)					Q index
				P <sub>1</sub>	P <sub>25</sub>	P <sub>50</sub>	P <sub>75</sub>	P <sub>99</sub>	
Conifers	<i>Pinus canariensis</i>	P1	903	351	536	768	1051	1388	0.305
	<i>Pinus halepensis</i>	M	526	422	500	543	559	558	0.063
	<i>Pinus nigra</i>	MXT3	944	1204	1064	941	832	737	0.123
	<i>Pinus pinaster</i>	MXT	1053	1353	1190	1046	920	809	0.129
	<i>Pinus pinea</i>	P4	683	700	632	756	982	1325	0.262
	<i>Pinus radiata</i>	PET3	1178	1355	1197	1116	1093	1120	0.058
	<i>Pinus sylvestris</i>	TAR	1146	1342	1241	1148	1063	984	0.078
	<i>Pinus uncinata</i>	PET3	1031	1109	1043	981	923	869	0.068
Broadleaves	<i>Fagus sylvatica</i>	MXT3	995	1188	1093	1005	924	850	0.085
	<i>Quercus faginea</i>	MXTWM	740	999	725	527	384	281	0.315
	<i>Quercus ilex</i>	PET3	319	496	409	337	278	229	0.211
	<i>Quercus petraea</i>	MXT	969	1268	1001	787	616	480	0.242
	<i>Quercus pyrenaica</i>	T4	840	1021	838	686	561	458	0.213
	<i>Quercus robur</i>	MNT3	787	993	888	790	699	616	0.120
	<i>Quercus suber</i>	PET3	585	721	608	512	432	364	0.176

453  
454  
455  
456

P - Percentile

457 Q indexes obtained for conifers (Tables 3, 4, 5) showed that the highest variations  
 458 in SDI<sub>max</sub> across different climatic conditions were obtained for *Pinus canariensis*

459 (0.305), followed by *Pinus pinea* (0.262). On the contrary, the lower values of Q  
460 index were found for *Pinus halepensis* (0.063) and *Pinus radiata* (0.058). Among  
461 broadleaf species, the lowest Q index was found for *Fagus sylvatica* (0.085) and  
462 the highest for *Quercus faginea* (0.315). The rest of the *Quercus* species  
463 presented similar values ranging from 0.11 to 0.24.

464

#### 465 **4.DISCUSSION**

466

467 In this study, a significant influence of climate on the MSDR was found for the 15  
468 Mediterranean species studied. Our results highlighted the need to consider  
469 different specific climatic variables to better predict this climatic influence as  
470 previous researchers (Aguirre et al. 2018; Condés et al. 2017; Brunet-Navarro et  
471 al. 2016; Charru et al., 2012). However, exact agreement with previously  
472 published studies (Aguirre et al. 2018; Brunet-Navarro et al. 2016) could not be  
473 expected for the same species and areas regarding the key drivers affecting the  
474 MSDR and the way they impact the maximum stand carrying capacity  
475 estimations. In addition, different approaches (Condés et al., 2017; Riofrio et al.  
476 2017) in selecting monospecific plots could derive in a different plot samples and  
477 therefore in different results. As well as this, regarding the climate database,  
478 although other databases could also be used such as Gonzalo Jimenez (2010),  
479 the most updated (1970-2000) time period offered by WorldClim2 available for  
480 the whole study area was selected in order to consider a suitable range of  
481 different climatic conditions with high resolution (Abatzoglou et al. 2018; Poggio  
482 et al. 2018; Panagos et al. 2017).

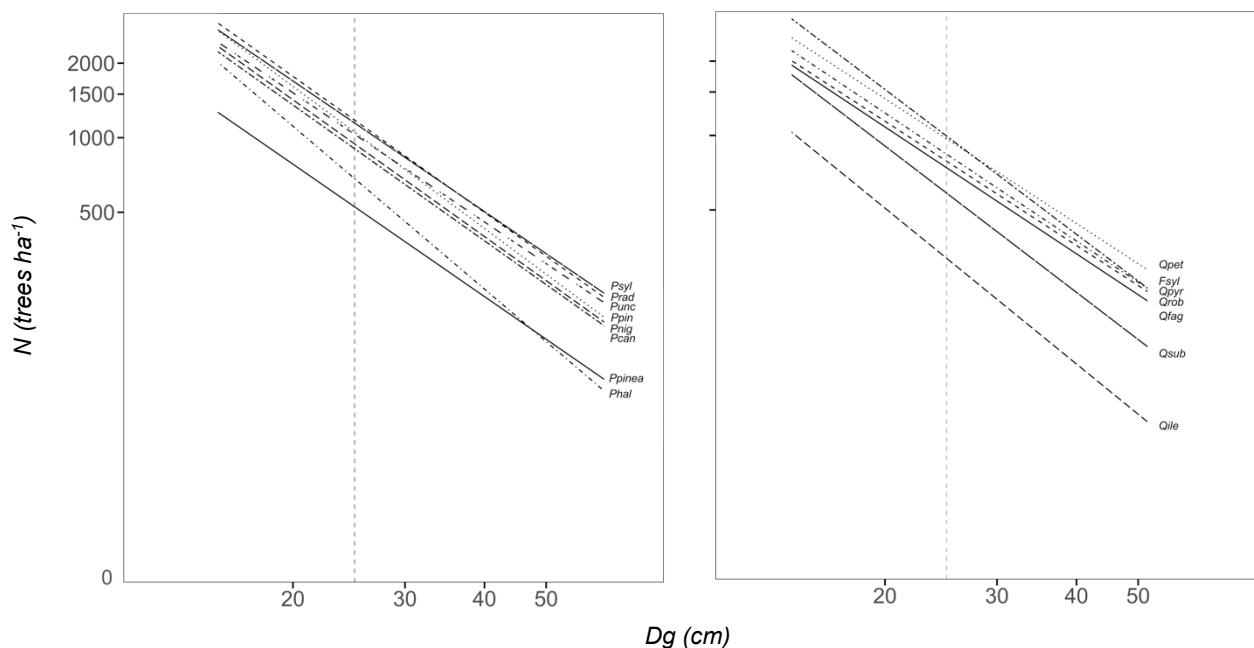
483

484 4.1. Basic MSDRs and  $SDI_{max}$  reference values

485

486 Our findings showed significant differences in the coefficients of the basic MSDRs  
487 (Tables 3 and 4), confirming intra- and inter-specific variability among the  
488 selected coniferous and broadleaf species (Vospernik and Sterba, 2015). The  
489 range of the slopes fitted in the basic MSDR models for the coniferous species  
490 agreed with findings reported by Charru et al. (2012) and Aguirre et al. (2018).  
491 Those authors found shallower slopes for *Pinus sylvestris* than for other pines in  
492 Spain and France, showing the great ability of this species to grow and survive  
493 amidst intra-specific competition (Zeide, 1987; Pretzsch and Biber, 2005). The  
494 development of wide crown areas at older ages could explain the extreme value  
495 of the slope for *Pinus pinea* (Barbeito et al., 2008). Among the broadleaf species,  
496 *Quercus suber* (-1.9674) and *Quercus ilex* (-2.0951) presented the steepest  
497 MSDR slopes and the smallest  $SDI_{max}$  estimates. These outputs may be due to  
498 the ability of these species to support a great leaf area, so that fewer individuals  
499 are needed to fully occupy a stand (Woodall et al., 2005).

500



501

502 **Figure 3:** Basic MSDR fits plotted on a log-log scale for the **(a)** coniferous and **(b)** broadleaf species  
503 studied.

504 *Note: Pcan - Pinus canariensis, Phal - Pinus halepensis, Pnig - Pinus nigra, Ppin - Pinus pinaster, Ppinea -*  
505 *Pinus pinea, Prad - Pinus radiata, Psyl - Pinus sylvestris, Punc - Pinus uncinata, Fsyl - Fagus sylvatica, Qfag -*  
506 *Quercus faginea, Qile - Quercus ilex, Qpet - Quercus petraea, Qpyr - Quercus pyrenaica, Qrob - Quercus*  
507 *robur, Qsub - Quercus suber*

508

509

510 The  $SDI_{maxREF}$  values estimated in this study were compared to prior reference  
511 values from published studies in similar areas, to test the consistency of our  
512 models (Table 6). Agreement was generally good, as stands dominated by  
513 conifers showed relatively higher  $SDI_{maxREF}$  values when compared to those  
514 dominated by broadleaf species. The distinct values obtained in other studies for  
515 the same species may be due to the use of different approaches, methodologies  
516 and datasets (Hann, 2014).  $SDI_{maxREF}$  values were obtained by quantile  
517 regression in this study, whereas other relevant studies used different  
518 methodologies and types of statistical analysis, such as stochastic frontier  
519 analysis (e.g. Charru et al., 2012) or simple linear regression (e.g. Brunet-  
520 Navarro et al., 2012). Our findings were consistent with the theory that maximum  
521 stand density is known to be positively related to species shade tolerance (Jack  
522 and Long 1996, Woodall et al., 2005). However,  $SDI_{maxREF}$  values for light-  
523 demanding coniferous species such as *Pinus pinaster*, *Pinus uncinata* and *Pinus*  
524 *sylvestris* were unexpectedly high (Table 5), given their low shade-tolerance  
525 (Niinemets and Valladares, 2006). A similar trend was found by Andrews et al.  
526 (2018), who obtained smaller  $SDI_{maxREF}$  values for shade-tolerant species such  
527 as *Fagus grandifolia* and *Acer saccharum* than other light-demanding species in  
528 the northeastern United States. Prior to that, Dixon and Keyser (2017) reported

529 similar results when analyzing the maximum stand density of 15 coniferous and  
530 broadleaf species in the same area. Higher maximum carrying capacities for light-  
531 demanding species such as *Pinus sylvestris* than for *Fagus sylvatica* or *Quercus*  
532 *petraea* were also obtained by Charru et al. (2012) and Toigo et al. (2018) in  
533 France. These results suggest the existence of other drivers affecting the  
534 maximum carrying capacity of the species studied, such as silvicultural  
535 objectives, plant phenology, crown allometry, available growing space or climate.

#### 536 4.2. Climatic influence on maximum stand carrying capacity

537 In this study, a significant influence of climate in the MSDR and the maximum  
538 stand carrying capacity of 15 Mediterranean tree species was found. Reductions  
539 in the maximum carrying capacity were generally linked to warmer and drier  
540 conditions, though the climatic drivers that best explained the influence of the  
541 climate on MSDR and  $SDI_{max}$  varied for conifer and broadleaf species.

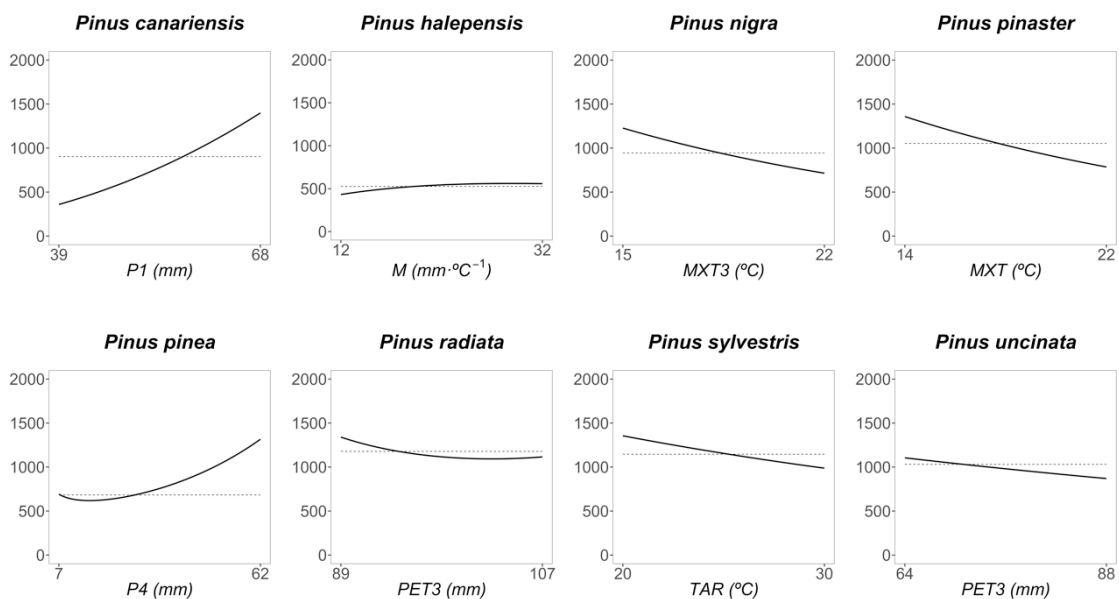
##### 542 4.2.1. Climatic influence on maximum stand carrying capacity for coniferous 543 species

544 Results from the climate-dependent MSDR models suggest that temperature  
545 could be the main driver affecting the maximum stand carrying capacity for  
546 conifers (Table 3). For *Pinus nigra*, *Pinus pinaster* and *Pinus sylvestris*, most of  
547 the selected climate-dependent models included seasonal temperatures,  
548 especially seasonal maximum (MXTi) temperatures.  $SDI_{max}$  (Clim) estimates for  
549 these species suggest that significant reductions in the maximum carrying  
550 capacity might be expected as temperatures increase, especially during the  
551 spring season (Figure 4). Contrary to this trend, recent research on climate  
552 change and coniferous forest dynamics (Martin-Benito et al., 2008; Kurz-Besson  
553 et al., 2016) suggest that reducing the number of days below 5°C could also

554 improve the growth and vitality of these species by enhancing processes such as  
555 winter photosynthesis (Rathgeber et al., 2005), cambium and xylem formation  
556 (Vieira et al., 2014) and the development of deeper roots during the colder  
557 months of the year (Hansen and Beck, 1994). An increase in minimum  
558 temperatures could also boost the growth of individuals in mountainous areas.  
559 Smaller snowpack has been linked to higher soil water availability (Kreyling,  
560 2010), lower mortality from root damage (Peterson and Peterson, 2001; Gedalof  
561 and Smith, 2001) and less foliar erosion from wind-blown snow (Kajimoto et al.,  
562 2002). The best climate-dependent models for *Pinus halepensis* indicated that  
563 seasonal maximum temperatures (MXT<sub>i</sub>), precipitation during the warmest month  
564 (PWM) and aridity (expressed as M) were the key drivers affecting SDI<sub>max</sub>. Small  
565 Q indexes were obtained for this species based on these models (Table 3),  
566 leading to small SDI<sub>max</sub> variations along its climatic range (Table 5). These results  
567 go in line with previous studies showing the high resilience and adaptation to  
568 extreme drought and heat conditions of this Mediterranean species (Baquedano  
569 and Castillo, 2007; Benito-Garzón et al., 2011; de Luis et al., 2013; Aguirre et al.  
570 2018). *Pinus uncinata* and *Pinus radiata* also showed small variations in SDI<sub>max</sub>  
571 (*Clim*) along their distribution area according to their best climate-dependent  
572 MSDR models and Q indexes (Table 5). Particularly, the best climate-dependent  
573 model (PET3) for *Pinus radiata* presented an atypical behavior in which SDI<sub>max</sub>  
574 (*Clim*) was found to decrease between percentiles 75 and 99 of this variable. This  
575 effect was also visible for *Pinus pinea*, which showed enhanced functioning at  
576 the highest values of P4. This might be explained by the link between climate and  
577 species traits, which is often too complex to adequately capture in a linear form  
578 (Reich, 2012; Craigmile, 2017). For this reason, further studies should test

579 alternative model structures (i.e. multiple regression) with different combinations  
 580 of climatic variables in order to better capture climate influences on MSDR and  
 581 SDI<sub>max</sub>. Results for *Pinus canariensis* and *Pinus pinea* revealed that seasonal (Pi)  
 582 and annual precipitation (P) seemed to be key variables affecting their maximum  
 583 stand carrying capacity. Indeed, these species showed the highest variation in  
 584 SDI<sub>max</sub> according to their Q index values (close to 0.3), suggesting that their  
 585 maximum stand carrying capacity would be very sensitive to potential changes in  
 586 precipitation regimes. In this context, climate change projections for the lower  
 587 areas of the Mediterranean basin emphasize that precipitation will continue to  
 588 decrease, especially during the warmest season (IPCC, 2018). Vitality (Sabaté  
 589 et al., 2002; Climent et al., 2006; Sanchez-Salguero et al., 2012), growth  
 590 reduction (Pasho et al., 2012; Gazol et al., 2017; Navarro-Cerillo et al., 2018;  
 591 Peña-Gallardo et al., 2018) and even death from xylem embolism (López et al.,  
 592 2013) due to increasing extreme drought events would be expected for  
 593 Mediterranean conifers and would indirectly influence the maximum number of  
 594 trees a stand could fully support in the future.

595  
 596



597  
 598

599 **Figure 4:** Climatic influence on the maximum stand carrying capacity (expressed as  $SDI_{max}$ ) for conifers.  
 600 Solid line corresponds to  $SDI_{max} (Clim)$  prediction estimates using the best climate-dependent MSDR model  
 601 by species. Dashed horizontal line represents the reference value of  $SDI_{maxREF}$ .

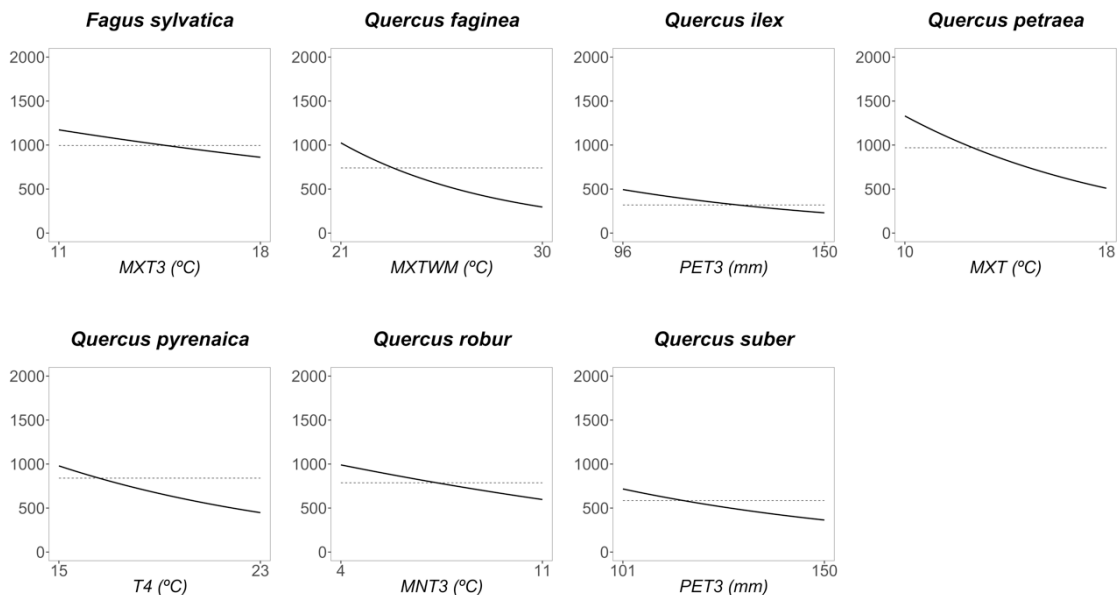
602 *Note: Temperature has been transformed to degrees Celsius (°C).*

603

604 **4.2.2. Climatic influence on maximum stand carrying capacity for broadleaf**  
 605 **species**

606 Similar to conifers, the influence of climate on MSDR was also found to be  
 607 significant for all broadleaf species (Table 4). Selected climate-dependent models  
 608 for *Fagus sylvatica* showed that higher  $SDI_{max}$  values were linked to wetter and  
 609 milder conditions (Table 4). This result corroborates results obtained previously  
 610 by Condés et al., (2017), who found a similar pattern when studying the influence  
 611 of aridity on MSDR in *Fagus sylvatica* and *Pinus sylvestris* stands across a wide  
 612 environmental gradient in Europe. Other studies (Friedrichs et al., 2009;  
 613 Zimmermann et al., 2015) on growth dynamics have reported similar climatic  
 614 impacts for this species.

615  
 616



617  
 618

619 **Figure 5:** Climatic influence on the maximum stand carrying capacity (expressed as  $SDI_{max}$ ) of broadleaf  
 620 species. Solid line corresponds to  $SDI_{max} (Clim)$  prediction estimates using the best climate-dependent  
 621 MSDR model by species. Dashed horizontal line represents the reference value,  $SDI_{maxREF}$ .

622 *Note: Temperature has been transformed to degrees Celsius (°C).*

623

624 For *Quercus* species, temperature was found to be the key driver affecting the  
625 maximum stand carrying capacity (Table 5). Based on the selected climate-  
626 dependent models by species, maximum temperatures in spring (MXT3) and  
627 summer (MXT4) influenced SDI<sub>max</sub> for all *Quercus* species except *Quercus robur*,  
628 which was more affected by potential changes in minimum temperatures (Table  
629 4). Similar to the results obtained for *Pinus* species, higher temperatures (both  
630 maximum and minimum) were linked to smaller SDI<sub>max</sub> estimates (Table 5). This  
631 is consistent with what has been found in previous studies (Fernandez-Marin et  
632 al., 2017; Gentilesca et al., 2017; Gil-Pelegrín et al., 2017; Kunz et al., 2018),  
633 suggesting that extreme heat and heat-induced drought conditions in the future  
634 would affect the vitality of oak stands in the Mediterranean basin. However,  
635 different responses in SDI<sub>max</sub> variation as effect of potential changes in  
636 temperature (Tables 4 and 5) were obtained among the *Quercus* species. The  
637 best climate-dependent models for *Quercus faginea* and *Quercus pyrenaica*  
638 suggest that a small increment in the temperatures of the warmest months would  
639 lead to a great decrease in the SDI<sub>max</sub> of this species (Figure 5). Indeed, *Quercus*  
640 *faginea* presented the highest Q index (0.315) among the studied oak species  
641 (Table 5) due to changes in MXTWM. Expected reductions in soil water reserves  
642 in the distribution area of this species could also foster its progressive substitution  
643 in the future by more drought-resistant species such as *Quercus suber* or  
644 *Quercus ilex* (Peñuelas et al., 2001). However, previous studies have revealed  
645 the great resilience and adaptability of *Quercus faginea* for surviving in extreme  
646 conditions, such as those expected in the Mediterranean Basin (Camarero et al.,  
647 2015). For this area, a pronounced warming is also predicted, giving rise to higher

648 rates of evapotranspiration with subsequent decreases in soil water availability  
649 and increases in drought episodes (IPCC,2018). Several authors have shown  
650 that these new conditions will drastically affect the growth and vitality of the main  
651 Mediterranean broadleaf species (Sabaté et al., 2002; Baquedano and Castillo,  
652 2007; Gea-Izquierdo et al. 2013; Gentilesca et al., 2017; Peña-Gallardo et al.,  
653 2018). In this context, different adaptation mechanisms such as leaf area  
654 reduction may be decisive for these oak species in order to reduce water loss  
655 and survive under these new conditions (Peguero-Pina et al., 2016). For *Quercus*  
656 *petraea*, maximum temperatures seemed to be also relevant climatic variables  
657 explaining potential reductions on the  $SDI_{max}$  (Figure 5) according to the best  
658 climate-dependent MSDR models obtained for this species (Table 4). Similar  
659 climatic influence was also reported by Michelot et al. (2012), who studied growth  
660 dynamics for *Quercus petraea* in France. However, positive impacts on growth  
661 (Kellomäki et al., 2008) and seed production (Caignard et al., 2017) could be  
662 expected in cold and mild areas, such as boreal and temperate forests, as an  
663 effect of global warming. As Spain is the western limit of *Quercus petraea*  
664 distribution, future climate change impacts could be more determinant for this oak  
665 species. As cited before, differences in  $SDI_{max}$  for *Quercus robur* could well be  
666 explained by changes in seasonal minimum temperatures (Table 4). However, a  
667 small climatic impact on  $SDI_{max}$  could be expected for this species linked to  
668 potential increments of minimum temperatures, according to its Q index (Table  
669 5). In this study, new climate-dependent MSDR models have been fitted and new  
670  $SDI_{maxREF}$  and  $SDI_{max}(Clim)$  for different broadleaf species have been estimated.  
671 However, further studies focused on these species are needed in order to better

672 understand and predict potential changes in the maximum stand carrying  
 673 capacity under different climate change scenarios.

674  
 675  
 676  
 677  
 678  
 679  
 680  
 681  
 682  
 683  
 684  
 685  
 686  
 687  
 688  
 689  
 690  
 691  
 692  
 693  
 694  
 695  
 696  
 697  
 698  
 699  
 700  
 701  
 702  
 703  
 704

**Table 6:** Comparison of the MSDR slope and SDI<sub>maxREF</sub> values obtained for the species studied in this paper and in similar works.

Functional Group	Species	$\beta_0$	SDI <sub>maxREF</sub>	Area	Statistical analysis	Reference
Conifers	<i>Pinus halepensis</i>	-1.881	637	France	SFA	Charru et al., 2012
		-1.777	732	Catalonia	SLR	Brunet-Navarro et al., 2016
		-1.829	619	Spain	QR (97.5 <sup>th</sup> percentile)	Aguirre et al., 2018
		-1.920	780	France	QR	Toigo et al., 2018
		<b>-1.776</b>	<b>526</b>	<b>Spain</b>	<b>QR (97.5<sup>th</sup> percentile)</b>	<b>This study</b>
	<i>Pinus nigra</i>	-1.653	881	France	SFA	Charru et al., 2012
		-1.787	600	Catalonia	SLR	Brunet-Navarro et al., 2016
		-1.794	960	Spain	QR (97.5 <sup>th</sup> percentile)	Aguirre et al., 2018
		-1.810	1181	France	QR	Toigo et al., 2018
		<b>-1.835</b>	<b>944</b>	<b>Spain</b>	<b>QR (97.5<sup>th</sup> percentile)</b>	<b>This study</b>
	<i>Pinus pinaster</i>	-1.711	648	France	SFA	Charru et al., 2012
		-1.929	1104	Spain	QR (95 <sup>th</sup> percentile)	Riofrio et al., 2016
		-1.983	1053	Spain	QR (97.5 <sup>th</sup> percentile)	Aguirre et al., 2018
		-1.860	807	France	QR	Toigo et al., 2018
		<b>-1.906</b>	<b>1053</b>	<b>Spain</b>	<b>QR (97.5<sup>th</sup> percentile)</b>	<b>This study</b>
	<i>Pinus pinea</i>	-1.857	1040	South Spain	SLR	Montero et al., 1998
		-2.122	702	Spain	QR (97.5 <sup>th</sup> percentile)	Aguirre et al., 2018
		<b>-2.186</b>	<b>683</b>	<b>Spain</b>	<b>QR (97.5<sup>th</sup> percentile)</b>	<b>This study</b>
<i>Pinus sylvestris</i>	-1.750	1444	Central Spain	NLR	Rio et al., 2001	
	-1.615	893	France	SFA	Charru et al., 2012	
	-1.750	1297	Navarra. Spain	NLR	Condés et al., 2013	

		-1.789	1144	Spain	QR (95 <sup>th</sup> percentile)	Riofrio et al., 2016
		-1.647	579	Catalonia. Spain	SLR	Brunet-Navarro et al., 2016
		-1.634	1078	Europe*	NLQR (97.5 <sup>th</sup> percentile)	Condés et al., 2017
		-1.726	1154	Spain	QR (97.5 <sup>th</sup> percentile)	Aguirre et al., 2018
		-2.020	1000	France	QR	Toigo et al., 2018
		<b>-1.752</b>	<b>1146</b>	<b>Spain</b>	<b>QR (97.5<sup>th</sup> percentile)</b>	<b>This study</b>
	<i>Pinus uncinata</i>	-1.665	581	Catalonia	SLR	Brunet-Navarro et al., 2016
		<b>-1.734</b>	<b>1031</b>	<b>Spain</b>	<b>QR (97.5<sup>th</sup> percentile)</b>	<b>This study</b>
	<i>Pinus canariensis</i>	<b>-1.823</b>	<b>903</b>	<b>Spain</b>	<b>QR (97.5<sup>th</sup> percentile)</b>	<b>This study</b>
	<i>Pinus radiata</i>	<b>-1.825</b>	<b>1178</b>	<b>Spain</b>	<b>QR (97.5<sup>th</sup> percentile)</b>	<b>This study</b>
Broadleaves	<i>Fagus sylvatica</i>	-1.941	814	France	SFA	Charru et al., 2012
		-1.943	1184	Europe*	NLQR (97.5 <sup>th</sup> percentile)	Condés et al., 2017
		-1.923	952	Spain	NLQR (97.5 <sup>th</sup> percentile)	Condés et al., 2017
		-1.790	991	France	QR	Toigo et al., 2018
		<b>-1.947</b>	<b>995</b>	<b>Spain</b>	<b>QR (97.5<sup>th</sup> percentile)</b>	<b>This study</b>
	<i>Quercus petraea</i>	-1.911	685	France	SFA	Charru et al., 2012
		-2.080	776	France	QR	Toigo et al., 2018
		<b>-1.678</b>	<b>969</b>	<b>Spain</b>	<b>QR (97.5<sup>th</sup> percentile)</b>	<b>This study</b>
	<i>Quercus robur</i>	-1.758	651	France	SFA	Charru et al., 2012
		-1.540	760	France	QR	Toigo et al., 2018
		<b>-1.670</b>	<b>787</b>	<b>Spain</b>	<b>QR (97.5<sup>th</sup> percentile)</b>	<b>This study</b>
	<i>Quercus faginea</i>	<b>-1.706</b>	<b>740</b>	<b>Spain</b>	<b>QR (97.5<sup>th</sup> percentile)</b>	<b>This study</b>
	<i>Quercus ilex</i>	<b>-2.095</b>	<b>319</b>	<b>Spain</b>	<b>QR (97.5<sup>th</sup> percentile)</b>	<b>This study</b>
	<i>Quercus pyrenaica</i>	<b>-1.720</b>	<b>840</b>	<b>Spain</b>	<b>QR (97.5<sup>th</sup> percentile)</b>	<b>This study</b>
	<i>Quercus suber</i>	<b>-1.967</b>	<b>585</b>	<b>Spain</b>	<b>QR (97.5<sup>th</sup> percentile)</b>	<b>This study</b>

Note: SFA – Stochastic Frontier Analysis; QR – Quantile Regression; NLQR – Non-Linear Quantile Regression; SLR – Simple Linear Regression; NLR – Non-Linear Regression  
\* Europe: Austria, France, Spain, Germany and Poland

705  
706  
707  
708  
709  
710

## 711 CONCLUSIONS

712

713 In this study, new reference and climate-dependent MSDR models and SDI<sub>max</sub>  
714 values are presented for 15 coniferous and broadleaf Mediterranean tree  
715 species. For all of them, a significant climatic influence on the MSDR and the  
716 maximum stand carrying capacity was found. Maximum temperatures, especially  
717 those related to spring and summer seasons, were found to be key drivers  
718 affecting the MSDR in most of the species studied. A general trend linking smaller  
719 SDI<sub>max</sub> values to warmer and drier conditions was found, suggesting that potential  
720 increments in temperatures and drought episodes would limit the maximum stand  
721 carrying capacity for these species. Climate impact on the maximum stand  
722 carrying capacity varied among species. However, according to the proposed Q  
723 index, the impact of climate on SDI<sub>max</sub> was found to be homogeneous among  
724 *Quercus* species, while conifers presented greater disparity. All the selected

725 climate-dependent models improved the goodness of fit over the basic models,  
726 highlighting the importance of using specific climatic variables to better  
727 characterize climatic impacts on MSDR. The climate-dependent MSDR models  
728 presented in this study will allow us to more precisely estimate maximum carrying  
729 capacity, providing an advanced tool for managing pure and mixed stands based  
730 on current and future climatic conditions in the Mediterranean Basin. Along these  
731 lines, further studies that include more tree species and a wider range of specific  
732 climatic conditions are necessary to better understand the complex interaction  
733 between climate and the potential stocking of Mediterranean forests.

734

735

#### 736 **CRedit AUTHOR STATEMENT**

737

738 Diego Rodríguez de Prado: Conceptualization, Methodology, Formal Analysis,  
739 Investigation, Data curation, Visualization, Writing-Original Draft, Writing –  
740 Review and Editing. Roberto San Martín: Formal analysis, Writing – Review and  
741 Editing. Felipe Bravo: Conceptualization, Writing – Review and Editing,  
742 Supervision. Celia Herrero de Aza: Conceptualization, Writing – Review and  
743 Editing, Supervision, Project administration.

744

#### 745 **DECLARATION OF COMPETING INTEREST**

746 The authors declare that they have no known competing financial interests or  
747 personal relationships that could have appeared to influence the work reported  
748 in this paper

749 **ACKNOWLEDGEMENTS**

750 The authors would like to thank the Spanish Ministry of Economy and  
751 Competitiveness for funding this research through Industrial PhD project [grant  
752 DI-15-07722] and the Torres Quevedo programme [grant PTQ-12-05409]. The  
753 authors are also grateful to the Ministry for Ecological Transition and the  
754 WorldClim team for sharing and providing the data used in this study. Finally, the  
755 authors would also thank Andrea Blanch for revising the manuscript and  
756 providing generous linguistic advice.

757

758 **REFERENCES**

759

760 Abatzoglou, J.T., Dobrowski, S.Z., Parks, S.A., Hegewisch, K.C., 2018. TerraClimate,  
761 a high-resolution global dataset of monthly climate and climatic water balance  
762 from 1958–2015. *Scientific Data* 5, Article number: 170191.

763

764 Aguirre, A., Del Rio, M., Condés, S., 2018. Intra- and inter-specific variation of  
765 the maximum size-density relationship along an aridity gradient in Iberian  
766 pinewoods. *For. Ecol. Manage.* 411, 90-100.

767

768 Alberdi, I., Sandoval, V., Condés, S., Cañellas, I., Vallejo, R., 2016. El Inventario  
769 Forestal Español, una herramienta para el conocimiento, la gestión y la  
770 conservación de los ecosistemas forestales arbolados. *Ecosistemas* 25, 88-96.

771

772 Andrews, C., Weiskittel, A., D'Amato, A.W., Simons-Legaard, E., 2018. Variation  
773 in the maximum stand density index and its linkage to climate in mixed species  
774 forests of the North American Acadian Region. *For. Ecol. Manage.* 417, 90-102.  
775

776 Baquedano, F.J., Castillo, F., 2007. Drought tolerance in the Mediterranean  
777 species *Quercus coccifera*, *Quercus ilex*, *Pinus halepensis*, and *Juniperus*  
778 *phoenicea*. *Photosynthetica* 45, 229.  
779

780 Barbeito, I., Pardos, M., Calama, R., Canellas, I., 2008. Effect of stand structure  
781 on Stone pine (*Pinus pinea* L.) regeneration dynamics. *Forestry* 81, 617–629.  
782

783 Bégin, E., Bégin, J., Bélanger, L., Rivest, L.P., Tremblay, St., 2001. Balsam fir  
784 self-thinning relationship and its constancy among different ecological regions.  
785 *Can. J. For. Res.* 31, 950-959.  
786

787 Benito-Garzón, M., Alía, R., Robson, T.M., Zavala, M.A., 2011. Intra-specific  
788 variability and plasticity influence potential tree species distributions under  
789 climate change. *Global. Ecol. Biogeogr.* 20, 766-778.  
790

791 Bielak, K., Dudzinska, M., Pretzsch, H., 2014. Mixed stands of Scots pine (*Pinus*  
792 *sylvestris* L.) and Norway spruce [*Picea abies* (L.) Karst] can be more productive  
793 than monocultures. Evidence from over 100 years of observation of long-term  
794 experiments. *For. Syst.* 23, 573–589.  
795

796 Bi, H., Wan, G., Turvey, N.D., 2000. Estimating the self- thinning boundary line  
797 as a density-dependent stochastic biomass frontier. *Ecology* 81, 1477-1483.

798 Bi, H., 2001. The self-thinning surface. *For. Sci.* 47, 361-370.

799

800 Bi, H., 2004. Stochastic frontier analysis of a classic self-thinning experiment.  
801 *Aust. Ecol.* 29, 408-417

802

803 Brunet-Navarro, P., Sterck, F.J., Vayreda, J., Martinez-Vilalta, J., Mohren, G.M.,  
804 2016. Self-thinning in four pine species: an evaluation of potential climate  
805 impacts. *Ann. Forest Sci.* 73, 1025-1034.

806

807 Caignard, T., Kremer, A., Firmat, C., Nicolas, M., Venner, S., Delzon, S., 2017.  
808 Increasing spring temperatures favor oak seed production in temperate areas.  
809 *Scientific Reports* 7, 8555.

810

811 Camarero, J.J., Franquesa, M., Sangüesa-Barreda, G., 2015. Timing of drought  
812 triggers distinct growth responses in holm oak: implications to predict warming-  
813 induced forest defoliation and growth decline. *Forests* 6, 1576-1597.

814

815 Charru, M., Seynave, I., Morneau, F., Rivoire, M., Bontemps, J.D., 2012.  
816 Significant differences and curvilinearity in the self-thinning relationships of 11  
817 temperate tree species assessed from forest inventory data. *Ann. Forest Sci.* 69,  
818 195-205.

819

820 Churchill, D.J., Larson, A.J., Dahlgreen, M.C., Franklin, J.F., Hessburg, P.F.,  
821 Lutz, J.A., 2013. Restoring forest resilience: from reference spatial patterns to  
822 silvicultural prescriptions and monitoring. *For. Ecol. Manage.* 291, 442-457.

823

824 Climent, J., Aranda, I., Alonso, J., Pardos, J., Gil, L., 2006. Developmental  
825 constraints limit the response of Canary Island pine seedlings to combined shade  
826 and drought. *For. Ecol. Manage.* 231, 164-168.

827

828 Comeau, P.G., White, M., Kerr, G., Hale, S.E., 2010. Maximum density-size  
829 relationships for Sitka spruce and coastal Douglas-fir in Britain and Canada.  
830 *Forestry* 83, 461-468.

831

832 Condés, S., del Río, M., Sterba, H., 2013. Mixing effect on volume growth of  
833 *Fagus sylvatica* and *Pinus sylvestris* is modulated by stand density. *For. Ecol.*  
834 *Manage.* 292, 86-95.

835

836 Condés, S., Vallet, P., Bielak, K., Bravo-Oviedo, A., Coll, L., Ducey, M.J., Pach,  
837 M., Pretzsch, H., Sterba, H., Vayreda, J., 2017. Climate influences on the  
838 maximum size- density relationship in Scots pine (*Pinus sylvestris* L.) and  
839 European beech (*Fagus sylvatica sylvatica* L.) stands. *For. Ecol. Manage.* 385,  
840 295-307.

841

842 Craigmile, P.F., Guttorp, P., 2017. Modeling and assessing climatic trends.  
843 Norwegian Computing Center eSACP:220730

844

845 de Luis, M., Čufar, K., Di Filippo, A., Novak, K., Papadopoulos, A., Piovesan, G.,  
846 Rathgeber, C.B.K., Raventós, J., Saz, M.A., Smith, K.T., 2013. Plasticity in  
847 Dendroclimatic Response across the Distribution Range of Aleppo Pine (*Pinus*  
848 *halepensis*). *PLoS ONE* 8, e83550

849

850 De Martonne, E., 1926. L'indice d'aridité. *Bulletin de l'Association de géographes*  
851 *français* 3, 3-5.

852

853 De Sampaio, C., Camilo-Alves, P., Esteves Da Clara, M.I., Cabral De Almeida  
854 Ribeiro, N.M., 2013. Decline of Mediterranean oak trees and its association with  
855 *Phytophthora cinnamomi*: a review. *Eur. J. For. Res.* 132, 411-432.

856

857 del Río, M., Condés, S., Pretzsch, H., 2014. Analyzing size-symmetric vs. size-  
858 asymmetric and intra-vs. inter-specific competition in beech (*Fagus sylvatica* L.)  
859 mixed stands. *For. Ecol. Manage.* 325, 90-98.

860

861 Dixon, G.E., Keyser, C.E., 2017. Northeast (NE) Variant Overview - Forest  
862 Vegetation Simulator. Internal Report. USDA, Forest Service, Forest Service  
863 Management Center, Ft. Collins, CO.

864

865 Drew, T., Flewelling, J.W., 1977. Some recent Japanese theories of yield-density  
866 relationships and their application to Monterey pine plantations. *For. Sci.* 23, 517-  
867 534.

868

869 Ducey, M.J., Knapp, R.A., 2010. A stand density index for complex mixed species  
870 forests in in the northeastern United States. *For. Ecol. Manage.* 260, 1613-1622.  
871

872 Ducey, M.J., Woodall, C.W., Bravo-Oviedo, A., 2017. Climate and species  
873 functional traits influence maximum live tree stocking in the Lake States, USA.  
874 *For. Ecol. Manage.* 386, 51-61.  
875

876 Fernandez-Marin, B., Hernández, A., Garcia-Plazaola, J.I., Esteban, R., Míguez,  
877 F., Artetxe, U., Gómez-Sagasti, M., 2017. Photoprotective Strategies of  
878 Mediterranean Plants in Relation to Morphological Traits and Natural  
879 Environmental Pressure: A Meta-Analytical Approach. *Front. Plant Sci.* 8.  
880

881 Fettig, C.J., Klepzig, K.D., Billings, R.F., Munson, A.S., Nebeker, T.E., Negrón,  
882 J.F., and Nowak, J.T., 2007. The effectiveness of vegetation management  
883 practices for prevention and control of bark beetle outbreaks in coniferous forests  
884 of the western and southern United States. *For. Ecol. Manage.* 238, 24-53.  
885

886 Fick, S.E., Hijmans, R.J., 2017. Worldclim 2: New 1-km spatial resolution climate  
887 surfaces for global land areas. *Int. J. Climatol.* 37, 4302-4315.  
888

889 Fowler, C.W., 1981. Density dependence as related to life history strategy. *Ecol.*  
890 *Soc. Am.* 62, 602-610.  
891

892 Freire, J.A., Rodrigues, G.C., Tomé, M., 2019. Climate Change Impacts on *Pinus*  
893 *pinaster* L. Silvicultural System for Cone Production and Ways to Contour Those

894 Impacts: A Review Complemented with Data from Permanent Plots. *Forests* 10,  
895 169.  
896  
897 Friedrichs, D.A., Trouet, V., Büntgen, U., Frank, D.C., Esper, J., Neuwirth, B.,  
898 Löffler, J., 2009. Species-specific climate sensitivity of tree growth in Central-  
899 West Germany. *Trees* 23, 729-739.  
900  
901 Gazol, A., Ribas, M., Gutiérrez, E., Camarero, J.J., 2017. Aleppo pine forests  
902 from across Spain show drought-induced growth decline and partial recovery.  
903 *Agric. For. Meteorol.* 232, 186-194.  
904  
905 Gea-Izquierdo, G., Fernández De Uña, L., Cañellas, I., 2013. Growth projections  
906 reveal local vulnerability of Mediterranean oaks with rising temperatures. *For.*  
907 *Ecol. Manage.* 305, 282-293.  
908  
909 Gedalof, Z., Smith, D.J., 2001. Dendroclimatic response of mountain hemlock  
910 (*Tsuga mertensiana*) in Pacific North America. *Can. J. For. Res.* 31, 322-332.  
911  
912 Gentilesca, T., Camarero, J. J., Colangelo, M., Nolè, A., and Ripullone, F., 2017.  
913 Drought-induced oak decline in the western Mediterranean region: an overview  
914 on current evidences, mechanisms and management options to improve forest  
915 resilience. *iFor. Biogeosci. For.* 10, 796-806.  
916  
917 Gil-Pelegrián, E., Saz, M.Á., Cuadrat, J.M., Peguero-Pina, J.J., Sancho-Knapik,  
918 D., 2017. Oaks Under Mediterranean-Type Climates: Functional Response to

919 Summer Aridity. In: Gil-Pelegrín E., Peguero-Pina J., Sancho-Knapik D. (eds)  
920 Oaks Physiological Ecology. Exploring the Functional Diversity of Genus  
921 Quercus L. *Tree Physiology* 7. Springer, Cham  
922

923 Hann, D.W., 2014. Modeling of the maximum size-density line and its trajectory  
924 line for tree species: Observations and opinions. *For. Biometrics Res. Pap.* 5.  
925 Oregon State University, College of Forestry. Corvallis, OR. pp. 33.  
926

927 Hansen, J., Beck, E., 1994. Seasonal changes in the utilization and turnover of  
928 assimilation products in 8-year-old Scots pine (*Pinus sylvestris* L.) trees. *Trees -*  
929 *Structure and Function* 8, 172-182.  
930

931 Herrero, C., Bravo, F., 2012. Can we get an operational indicator of forest carbon  
932 sequestration? A case study from two forest regions in Spain. *Ecol. Indicators.*  
933 17, 120-126.  
934

935 Hutchings, M.J., Budd, C.S., 1981. Plant competition and its course through time.  
936 *BioScience* 3, 640-645.  
937

938 IPCC, 2018. Global Warming of 1.5°C. An IPCC Special Report on the impacts  
939 of global warming of 1.5°C above pre-industrial levels and related global  
940 greenhouse gas emission pathways, in the context of strengthening the global  
941 response to the threat of climate change, sustainable development, and efforts  
942 to eradicate poverty [Masson-Delmotte, V., P. Zhai, H.-O. Pörtner, D. Roberts, J.  
943 Skea, P.R. Shukla, A. Pirani, Moufouma-Okia, C. Péan, R. Pidcock, S. Connors,

944 J.B.R. Matthews, Y. Chen, X. Zhou, M.I. Gomis, E. Lonnoy, Maycock, M. Tignor,  
945 and T. Waterfield (eds.)). World Meteorological Organization, Geneva,  
946 Switzerland, 32 pp.

947

948 Jack, S.B., Long, J.N., 1996. Linkages between silviculture and ecology: An  
949 analysis of density management diagrams. *For. Ecol. Manage.* 86, 205-220.

950

951 Kajimoto, T., Seki, T., Ikeda, S., Daimaru, H., Okamoto, T., Onodera, H., 2002.  
952 Effects of snowfall fluctuation on tree growth and establishment of subalpine  
953 *Abies mariesii* near upper forest-limit of Mt. Yumori, northern Japan. *Arct. Antarct.*  
954 *Alp. Res.* 34, 191-200.

955

956 Kellomäki, S., Peltola, H., Nuutinen, T., Korhonen, K. T., & Strandman, H., 2008.  
957 Sensitivity of managed boreal forests in Finland to climate change, with  
958 implications for adaptive management. *Philosophical transactions of the Royal*  
959 *Society of London. Series B, Biological sciences* 363, 2341-2351.

960

961 Kimsey, M.J., Shaw, T.M., Coleman, M.D., 2019. Site sensitive maximum stand  
962 density index models for mixed conifer stands across the Inland Northwest, USA.  
963 *For. Ecol. Manage.* 433, 396-404.

964

965 Koenker, R., Bassett, G., 1978. Regression quantiles. *Econometrica* 46, 33-50.

966

967 Koenker, R., Machado, J.A., 1999. Goodness of fit and related inference  
968 processes for quantile regression. *J. Am. Statist. Assoc.* 94, 1296-1310.

969

970 Koenker, R., 2015. quantreg: Quantile Regression. R package version 5.05. R

971 Foundation for Statistical Computing: Vienna. Available at: [http://CRAN.R-](http://CRAN.R-project.org/package=quantreg)

972 [project.org/package=quantreg](http://CRAN.R-project.org/package=quantreg).

973

974 Kreyling, J., 2010. Winter climate change: a critical factor for temperate

975 vegetation performance. *Ecology* 91, 1939-1948.

976

977 Kreyling, J., Schmid, S., Aas, G., 2015. Cold tolerance of tree species is related

978 to the climate of their native ranges. *J. Biogeography*. 42, 156-166.

979

980 Kunz, J., Räder, A., Bauhus, J., 2018. Minor European broadleaved tree species

981 are more drought-tolerant than *Fagus sylvatica* but not more tolerant than

982 *Quercus petraea*. *For. Ecol. Manage.* 414, 15-27.

983

984 Kurz-Besson, C.B., Lousada, J.L., Gaspar, M.J., Correia, I.E., David, T.S.,

985 Soares, P.M., Cardoso, R.M., Russo, A., Varino, F., Mériaux, C., Trigo, R.M.,

986 Gouveia, C.M., 2016. Effects of Recent Minimum Temperature and Water Deficit

987 Increases on *Pinus pinaster* Radial Growth and Wood Density in Southern

988 Portugal. *Front. Plant Sci.* 7, 1170.

989

990 Kweon, D., Comeau, P.G., 2017. Effects of climate on maximum size-density

991 relationships in Western Canadian trembling aspen stands. *For. Ecol. Manage.*

992 406, 281-289.

993

994 Long, J.N., Shaw, J.D., 2005. A density management diagram for even-aged  
995 ponderosa pine stands. *West. J. Appl. For.* 20, 205-215.  
996

997 López, R., López de Heredia, U., Collada, C., Cano, F.J., Emerson, B.C.,  
998 Cochard, H., Gil, L., 2013. Vulnerability to cavitation, hydraulic efficiency, growth  
999 and survival in an insular pine (*Pinus canariensis*). *Ann Bot.* 111, 1167-1179.  
1000

1001 Makela, A., Landsberg, J., Ek, A.R., Burk, T.E., Ter-Mikaelian, M., Agren, G.I.,  
1002 Oliver, C.D., Puttonen, P., 2000. Process-based models for forest ecosystem  
1003 management: current state of the art and challenges for practical implementation.  
1004 *Tree Physiol.* 20, 289-298.  
1005

1006 Michelot, A., Simard, S., Rathgeber, C., Dufrêne, E., Damesin, C., 2012.  
1007 Comparing the intra-annual wood formation of three European species (*Fagus*  
1008 *sylvatica*, *Quercus petraea* and *Pinus sylvestris*) as related to leaf phenology and  
1009 non-structural carbohydrate dynamics. *Tree Physiol.* 32, 1033-1045.  
1010

1011 Montero, G., Candela, J., Gutiérrez, M., Pavón, J., Ortega, C., García, C.,  
1012 Cañellas, I., 1998. Manual de claras para repoblaciones de *Pinus pinea* L.  
1013 Editado por EGMASA y Junta de Andalucía.  
1014

1015 Moore, M.M., Deiter, D.A., 1992. Stand density index as a predictor of forage  
1016 production in northern Arizona ponderosa pine forests. *J. Range Manage.* 45,  
1017 267-271.  
1018

1019 Morris, C.E., 2003. How does fertility of the substrate affect intraspecific  
1020 competition? Evidence and synthesis from self-thinning. *Ecol. Res.* 18, 287-305.  
1021

1022 Navarro-Cerrillo, R.M., Rodríguez-Vallejo, C., Silveiro, E., Hortal, A.A., Palacios-  
1023 Rodríguez, G., Duque-Lazo, J., Camarero, J.J., 2018. Cumulative Drought Stress  
1024 Leads to a Loss of Growth Resilience and Explains Higher Mortality in Planted  
1025 than in Naturally Regenerated *Pinus pinaster* Stands. *Forests* 9, 358.  
1026

1027 Niinemets, Ü., Valladares, F., 2006. Tolerance to shade, drought, and  
1028 waterlogging of temperate northern hemisphere trees and shrubs. *Ecol. Monogr.*  
1029 76, 521-547.  
1030

1031 Panagos, P., Borrelli, P., Meusburger, K., Yu, B., Klik, A., Lim, K., Yang, J., Ni, J., Miao,  
1032 C., Chattopadhyay, N., Sadeghi, S.H., Hazbavi, Z., Zabihi, M., Larionov, G., Krasnov,  
1033 S., Gorobets, A., Levi, Y., Erpul, G., Birkel, C., Ballabio, C., 2017. Global rainfall  
1034 erosivity assessment based on high-temporal resolution rainfall records.  
1035 *Scientific Reports* 7, Article Number 4175.  
1036

1037 Pasho, E., Camarero, J.J., Vicente-Serrano, S.M., 2012. Climatic impacts and  
1038 drought control of radial growth and seasonal wood formation in *Pinus*  
1039 *halepensis*. *Trees* 26, 1875-1886.  
1040

1041 Peguero-Pina, J.J., Sisó, S., Sancho-Knapik, D., Díaz-Espejo, A., Flexas, J.,  
1042 Galmés, J., Gil-Pelegrín, E., 2016. Leaf morphological and physiological  
1043 adaptations of a deciduous oak (*Quercus faginea* Lam.) to the Mediterranean

1044 climate: a comparison with a closely related temperate species (*Quercus robur*  
1045 L.). *Tree Physiol.* 36, 287-99.

1046

1047 Peña-Gallardo, M., Vicente-Serrano, S.M., Camarero, J.J., Gazol, A. ; Sánchez-  
1048 Salguero, R.; Domínguez-Castro, F., El-Kenawy, A.M., Beguería, S.; Gutiérrez,  
1049 E., de-Luis,M., Sangüesa-Barreda, G., Novak, K.; Rozas, V., Tíscar, P.A.,  
1050 Linares, J.C., Martínez-del-Castillo, E., Ribas-Matamoros, M., García-González,  
1051 I; Silla, F., Camisón, A., Génova, M., Olano, J.M., Longares, L.A., Hevia, A.,  
1052 Galván, D., 2018. Drought Sensitiveness on Forest Growth in Peninsular Spain  
1053 and the Balearic Islands. *Forests* 2018, 9, 524.

1054

1055 Peñuelas, J., Lloret, F., Montoya, R., 2001. Severe drought effects on  
1056 Mediterranean woody flora of Spain. *For. Sci.* 47, 214-218.

1057

1058 Perez-Sierra, A., Lopez-Garcia, C., Leon, M., Garcia-Jimenez, J., Abad-Campos,  
1059 P., Jung, T., 2013. Previously unrecorded low-temperature *Phytophthora* species  
1060 associated with *Quercus* decline in a Mediterranean forest in eastern Spain.  
1061 *Forest Pathology* 43, 331-339.

1062

1063 Peterson, D.W., Peterson, D.L., 2001. Mountain hemlock growth responds to  
1064 climatic variability at annual and decadal time scales. *Ecology* 82, 3330-3345.

1065

1066 Poggio,L., Simonetti,E., Gimona,A., 2018. Enhancing the WorldClim data set for  
1067 national and regional applications. *Science of the Total Environment* 625,1628-  
1068 1643.

1069

1070 Pretzsch, H., Biber, P., 2005. A re-evaluation of Reineke's rule and stand density  
1071 index. *For. Sci.* 51, 304-320.

1072

1073 Pretzsch, H., Biber, P., 2016. Tree species mixing can increase maximum stand  
1074 density. *Can. J. For. Res.* 46, 1179-1193.

1075

1076 R Core Team, 2018. R: A language and environment for statistical computing. R  
1077 Foundation for Statistical Computing, Vienna, Austria. URL [https://www.R-](https://www.R-project.org/)  
1078 [project.org/](https://www.R-project.org/).

1079

1080 Rathgeber, C.B.K., Misson, L., Nicault, A., Guiot, J., 2005. Bioclimatic model of  
1081 tree radial growth: Application to the French Mediterranean Aleppo pine forests.  
1082 *Trees* 19, 162-176.

1083

1084 Ratwosky, D.A., 1983. Nonlinear regression modeling. A unified practical  
1085 approach. Marcel Dekker Inc., New York

1086

1087 Reich, B.J., 2012. Spatiotemporal quantile regression for detecting distributional  
1088 changes in environmental processes. *Journal of the Royal Statistical Society:*  
1089 *Series C (Applied Statistics)* 61, 535-553.

1090

1091 Reineke, L.H., 1933. Perfecting a stand-density index for even-aged forests. *J.*  
1092 *Agric. Res.* 46, 627-638.

1093

1094 Reyes-Hernandez, V., Comeau, P.G., Bokalo, M., 2013. Static and dynamic  
1095 maximum size- density relationships for mixed trembling aspen and white spruce  
1096 stands in western Canada. *For. Ecol. Manage.* 289, 300-311.  
1097

1098 Rio, M., Montero, G., Bravo, F., 2001. Analysis of diameter-density relationships  
1099 and self- thinning in non-thinned even-aged Scots pine stands. *For. Ecol.*  
1100 *Manage.* 142, 79-87.  
1101

1102 Riofrío, J., del Río, M., Bravo, F., 2016. Mixing effects on growth efficiency in  
1103 mixed pine forests. *Forestry* 90, 381-392.

1104 Sabaté, S., Gracia, C. A., Sánchez, A., 2002. Likely effects of climate change on  
1105 growth of *Quercus ilex*, *Pinus halepensis*, *Pinus pinaster*, *Pinus sylvestris* and  
1106 *Fagus sylvatica* forests in the Mediterranean region. *For. Ecol. Manage.*, 162, 23-  
1107 37.  
1108

1109 Sánchez-Salguero, R., Navarro-Cerrillo, R.M., Swetnam, T.W., Zavala, M.A.,  
1110 2012. Is drought the main decline factor at the rear edge of Europe? The case of  
1111 southern Iberian pine plantations. *For. Ecol. Manage.* 271, 158-169.  
1112

1113 Serrada, R., Montero, G., Reque, J.A., 2008. Compendio de selvicultura aplicada  
1114 en España. INIA - Fundación Conde del Valle de Salazar, Spain, pp. 178.  
1115

1116 Toigo, M., Perot, T., Courbaud, B., Castagneyrol, B., Gégout, J.C., Longuetaud,  
1117 F., Jactel, H., Vallet, P., 2018. Difference in shade tolerance drives the mixture  
1118 effect on oak productivity. *J. Ecol.* 106, 1073-1082.

1119

1120 Trabucco, A., Zomer, R.J., 2009. Global Aridity Index (Global-Aridity) and Global  
1121 Potential Evapo-Transpiration (Global-PET) Geospatial Database. CGIAR  
1122 Consortium for Spatial Information. Published online, available from the CGIAR-  
1123 CSI GeoPortal at: <http://www.csi.cgiar.org>

1124

1125 Valbuena, P., Del Peso, C., Bravo, F., 2008. Stand density Management  
1126 diagrams for two mediterranean pine species in Eastern Spain. *Forest Syst.* 17,  
1127 97-104.

1128

1129 Vieira, J., Rossi, S., Campelo, F., Freitas, H., Nabais, C., 2014. Xylogenesis of  
1130 *Pinus pinaster* under a Mediterranean climate. *Ann. For. Sci.* 71, 71-80.

1131

1132 Vospernik, S., Sterba, H., 2015. Do competition-density rule and self-thinning rule  
1133 agree? *Ann. Forest Sci.* 72, 379-390.

1134

1135 Weiskittel, A., Gould, P., Temesgen, H., 2009. Sources of variation in the self-  
1136 thinning boundary line for three species with varying levels of shade tolerance.  
1137 *For. Sci.* 55, 84-93.

1138

1139 Weller, D.E., 1987. A reevaluation of the  $-3/2$  % power rule of plant self-thinning.  
1140 *Ecol. Monogr.* 57, 23-43.

1141

1142 Woodall, C.W., D'Amato, A.W., Bradford, J.B., Finley, A.O., 2011. Effects of  
1143 stand and inter-specific stocking on maximizing standing tree carbon stocks in  
1144 the Eastern United States. *For. Sci.* 57, 365-378.  
1145  
1146 Woodall, C.W., Miles, P.D., Vissage, J.S., 2005. Determining maximum stand  
1147 density index in mixed species stands for strategic-scale stocking assessments.  
1148 *For. Ecol. Manage.* 216, 367-377.  
1149  
1150 Yang, Y., Titus, S.J., 2002. Maximum size-density relationships for constraining  
1151 individual tree mortality functions. *For. Ecol. Manage.* 168, 259-273.  
1152  
1153 Yoda, K., Kira, T., Ogawa, H., Hozumi, K., 1963. Self-thinning in overcrowded  
1154 pure stands under cultivated and natural conditions (Intraspecific competition  
1155 among higher plants XI). *J. Biol.* 14, 107-129.  
1156  
1157 Zeide, B., 1985. Tolerance and self-tolerance of trees. *For. Ecol. Manage.* 13,  
1158 149-166.  
1159  
1160 Zeide, B., 1987. Analysis of the 3/2 power law of self-thinning. *Forest Sci.* 33,  
1161 517-537.  
1162  
1163 Zeide, B., 2005. How to measure stand density. *Trees - Struct. Funct.* 19, 1-14.  
1164

1165 Zhang, L.J., Bi, H.Q., Gove, J.H., Heath, L.S., 2005. A comparison of alternative  
1166 methods for estimating the self-thinning boundary line. *Can. J. For. Res.* 35,  
1167 1507-1514.

1168

1169 Zhang, J., Oliver, W.W., Powers, R.F., 2013. Reevaluating the self-thinning  
1170 boundary line for ponderosa pine (*Pinus ponderosa*) forests. *Can. J. For. Res.*  
1171 43, 963-971.

1172

1173 Zimmermann, J., Hauck, M., Dulamsuren, C., Leuschner, C.J., 2015. Climate  
1174 Warming-Related Growth Decline Affects *Fagus sylvatica*, But Not Other Broad-  
1175 Leaved Tree Species in Central European Mixed Forests. *Ecosystems* 18, 560-  
1176 572.

1177

1178

1179 **Supplementary material**

**Supplementary Table 1** Mean  $\pm$  standard deviation and range (minimum-maximum) of the climatic variables used to fit the climate-dependent MSDR models for coniferous species

	<i>Pinus canariensis</i>	<i>Pinus halepensis</i>	<i>Pinus nigra</i>	<i>Pinus pinea</i>	<i>Pinus pinaster</i>	<i>Pinus radiata</i>	<i>Pinus sylvestris</i>	<i>Pinus uncinata</i>
<b>Plots</b>	1158	6074	2321	4427	1352	874	4082	385
<b>T (°C)</b>	14.1 $\pm$ 1.8 (10-18.9)	14.1 $\pm$ 1.5 (10.5-18.1)	10.7 $\pm$ 1.1 (6.7-14.3)	12.4 $\pm$ 1.6 (7.9-17.4)	14.7 $\pm$ 2 (11.3-18.1)	12.6 $\pm$ 0.9 (9.5-17.2)	8.7 $\pm$ 1.4 (3.6-13.7)	5.2 $\pm$ 1 (2.5-7.7)
<b>T1 (°C)</b>	13.3 $\pm$ 2.1 (7.9-18.9)	10.4 $\pm$ 1.9 (6.4-16)	7.3 $\pm$ 1.2 (3.6-11)	9.2 $\pm$ 2 (4.7-15.2)	11.2 $\pm$ 2.5 (7.6-16.4)	10.7 $\pm$ 1.2 (7-17.2)	5.9 $\pm$ 1.4 (1.5-10.4)	3 $\pm$ 0.9 (0.7-5.3)
<b>T2 (°C)</b>	10.4 $\pm$ 2.1 (5.2-16.1)	7.7 $\pm$ 1.7 (3.4-12.6)	4.3 $\pm$ 1.2 (0.3-8.3)	6.6 $\pm$ 2.1 (1.6-12.3)	8.6 $\pm$ 2.4 (4.9-13.2)	7.9 $\pm$ 1.2 (4.2-14.2)	2.8 $\pm$ 1.5 (-1.8-7.7)	-0.1 $\pm$ 0.9 (-2.5-2.5)
<b>T3 (°C)</b>	13.8 $\pm$ 1.7 (10.2-18.3)	15.9 $\pm$ 1.3 (12.2-19.3)	12.1 $\pm$ 1.2 (7.1-15.9)	13.7 $\pm$ 1.6 (8.9-18.5)	16.3 $\pm$ 1.8 (12.9-19.2)	13.3 $\pm$ 0.7 (10.6-16.7)	9.8 $\pm$ 1.6 (3.1-15.4)	5.3 $\pm$ 1.3 (1.5-8.4)
<b>T4 (°C)</b>	19 $\pm$ 1.3 (16-22.7)	22.5 $\pm$ 1.3 (18.4-25.5)	19.1 $\pm$ 1.3 (13.2-23.1)	19.9 $\pm$ 1.9 (15.9-25.3)	22.7 $\pm$ 1.8 (19.5-25.7)	18.3 $\pm$ 0.7 (15.7-22)	16.4 $\pm$ 1.3 (11.1-21.3)	12.6 $\pm$ 1.1 (9.5-15.2)
<b>MNT (°C)</b>	10.5 $\pm$ 1.8 (6.2-15.6)	8.2 $\pm$ 1.9 (3.9-13.6)	5 $\pm$ 1.2 (1.8-9)	7.2 $\pm$ 2 (2.4-13.8)	9.1 $\pm$ 2.3 (5.4-14.7)	8.6 $\pm$ 1 (5.4-13.9)	4 $\pm$ 1.3 (0.2-8.5)	1.7 $\pm$ 0.8 (-0.6-3.9)
<b>MNT1 (°C)</b>	9.9 $\pm$ 2.2 (5.1-15.8)	5.6 $\pm$ 2.2 (1.4-12.6)	2.6 $\pm$ 1.2 (-0.3-7.5)	5 $\pm$ 2.3 (0.2-11.6)	6.6 $\pm$ 2.6 (2.8-13.1)	7.3 $\pm$ 1.2 (3.4-14.4)	2 $\pm$ 1.2 (-1.6-9)	0.4 $\pm$ 0.7 (-1.8-2.5)
<b>MNT2 (°C)</b>	6.4 $\pm$ 2.2 (0.6-12.8)	0.7 $\pm$ 2.4 (-4.6-8.2)	-2.3 $\pm$ 1.6 (-6.8-3.6)	0.5 $\pm$ 3 (-5.5-8.7)	2 $\pm$ 3 (-2.1-10)	3.4 $\pm$ 1.5 (-0.4-10.4)	-2.7 $\pm$ 1.5 (-7.5-3.6)	-4.5 $\pm$ 1.2 (-7.7--1.6)
<b>MNT3 (°C)</b>	9.8 $\pm$ 1.7 (5.6-15)	8.9 $\pm$ 1.8 (4.2-14.3)	5.5 $\pm$ 1.5 (1.6-10)	7.6 $\pm$ 2 (2.1-14.5)	9.7 $\pm$ 2.2 (6-15.3)	8.8 $\pm$ 0.9 (5.7-12.8)	4.2 $\pm$ 1.5 (-0.6-9.4)	0.9 $\pm$ 1 (-1.5-3.4)
<b>MNT4 (°C)</b>	15.7 $\pm$ 1.3 (13.3-19)	17.7 $\pm$ 1.5 (13.2-21)	14.3 $\pm$ 1.2 (10.6-18)	15.6 $\pm$ 1.7 (12.1-20.2)	18.1 $\pm$ 1.8 (14.6-20.6)	14.9 $\pm$ 0.6 (12.4-18.1)	12.5 $\pm$ 1.1 (8.9-16.9)	9.9 $\pm$ 0.8 (7.9-12.2)
<b>MXT (°C)</b>	17.8 $\pm$ 1.8 (12.9-22.7)	20 $\pm$ 1.3 (16-23.8)	16.4 $\pm$ 1.3 (9.9-20.1)	17.6 $\pm$ 1.6 (12.7-23.2)	20.3 $\pm$ 1.9 (16.9-24)	16.6 $\pm$ 0.9 (13.5-20.6)	13.5 $\pm$ 1.7 (6.2-18.9)	8.7 $\pm$ 1.4 (4.7-12.2)
<b>MXT1 (°C)</b>	16.6 $\pm$ 2.1 (10.7-22.2)	15.3 $\pm$ 1.7 (11.1-20.9)	12 $\pm$ 1.3 (6.9-15.6)	13.5 $\pm$ 1.7 (8.3-18.8)	15.9 $\pm$ 2.5 (11.8-20.4)	14.1 $\pm$ 1.2 (10.3-20.3)	9.8 $\pm$ 1.7 (3.4-14.9)	5.6 $\pm$ 1.3 (2.2-9.1)
<b>MXT2 (°C)</b>	14.4 $\pm$ 2.1 (9-19.8)	14.6 $\pm$ 1.4 (10.2-18.4)	11 $\pm$ 1.2 (5.5-14.3)	12.7 $\pm$ 1.6 (7.3-18)	15.2 $\pm$ 2 (11.3-19.2)	12.5 $\pm$ 1.1 (8.7-18.1)	8.4 $\pm$ 1.7 (1.9-13.6)	4.3 $\pm$ 1.1 (1.1-7.1)
<b>MXT3 (°C)</b>	17.9 $\pm$ 1.8 (12.9-22.8)	22.8 $\pm$ 1.4 (17.5-26.1)	18.8 $\pm$ 1.4 (10.9-23.4)	19.9 $\pm$ 1.9 (14.5-26)	22.8 $\pm$ 1.7 (19.1-26.5)	17.9 $\pm$ 0.9 (14.4-21.7)	15.3 $\pm$ 2 (6.5-21.4)	9.7 $\pm$ 1.8 (4.5-13.7)
<b>MXT4 (°C)</b>	22.3 $\pm$ 1.4 (17.9-26.7)	27.4 $\pm$ 1.3 (22.4-30.8)	23.8 $\pm$ 1.6 (15.9-28.2)	24.1 $\pm$ 2.2 (19.2-30.7)	27.4 $\pm$ 1.9 (23.7-30.9)	21.7 $\pm$ 0.8 (18.7-26.5)	20.3 $\pm$ 1.7 (13.1-26.1)	15.2 $\pm$ 1.6 (10.9-19)
<b>MXTWM (°C)</b>	23.1 $\pm$ 1.4 (18.7-27.3)	28.8 $\pm$ 1.3 (23.5-32.1)	25.3 $\pm$ 1.8 (17-30)	25.3 $\pm$ 2.5 (20-32.1)	28.7 $\pm$ 1.9 (24.9-32.3)	22.4 $\pm$ 0.8 (19.7-27.7)	21.5 $\pm$ 1.7 (14.6-27.2)	16.5 $\pm$ 1.5 (12.3-20.3)
<b>MNTCM (°C)</b>	5.9 $\pm$ 2.4 (-0.1-12.6)	-0.9 $\pm$ 2.7 (-6.1-7.6)	-3.8 $\pm$ 1.5 (-8.1-2.9)	-1 $\pm$ 3.2 (-7-7.8)	0.3 $\pm$ 3.3 (-4.1-9)	2.5 $\pm$ 1.7 (-1.9-10.2)	-3.9 $\pm$ 1.3 (-8.2-3)	-5 $\pm$ 1.2 (-8.2-2.1)
<b>TAR (°C)</b>	290.3 $\pm$ 2 (285.2-294.6)	302.7 $\pm$ 2.9 (289.3-307.3)	302 $\pm$ 2.3 (291.9-307.2)	299.3 $\pm$ 4.8 (287.6-307.1)	301.4 $\pm$ 3 (291.8-306.4)	293 $\pm$ 1.7 (285.9-299.6)	298.4 $\pm$ 1.9 (290.6-305)	294.6 $\pm$ 1.8 (291.4-299.1)
<b>P (mm)</b>	406.8 $\pm$ 46.2 (258-516)	453.8 $\pm$ 99.6 (273-868)	599.6 $\pm$ 126.4 (373-1364)	769.9 $\pm$ 436.5 (329-1988)	489.4 $\pm$ 108.9 (326-891)	1120.2 $\pm$ 214.7 (318-1802)	799.6 $\pm$ 187.9 (393-1597)	1222.4 $\pm$ 109.8 (683-1474)
<b>P1 (mm)</b>	54.5 $\pm$ 6.7 (34.3-69.3)	48.6 $\pm$ 13.2 (28-109.7)	59.7 $\pm$ 13.6 (28.3-149.7)	90 $\pm$ 55.4 (30.3-252)	61.3 $\pm$ 17.6 (36.3-121.3)	116.8 $\pm$ 25.2 (46-211.7)	80.7 $\pm$ 23.2 (31-190.7)	121.9 $\pm$ 12.4 (59-153)
<b>P2 (mm)</b>	59.5 $\pm$ 7.3 (37-75.7)	35.5 $\pm$ 12.2 (18-119.7)	45.8 $\pm$ 13.6 (17-128)	76 $\pm$ 53.2 (20-236.7)	45.6 $\pm$ 16.6 (24-136.3)	100.8 $\pm$ 22.6 (45-213)	63 $\pm$ 19.7 (21.7-171.3)	96.8 $\pm$ 11.6 (47.7-124)
<b>P3 (mm)</b>	15.5 $\pm$ 1.7 (9.7-19.7)	42.6 $\pm$ 8.9 (15.7-81.7)	59.8 $\pm$ 11 (39-115.3)	60.5 $\pm$ 23.4 (30-128.3)	39.6 $\pm$ 7.4 (27.3-76.3)	91.3 $\pm$ 18 (10-119.3)	76.1 $\pm$ 13.6 (40-122)	110 $\pm$ 8.8 (77-129.7)
<b>P4 (mm)</b>	6.2 $\pm$ 0.9 (3.7-9.7)	24.6 $\pm$ 12.1 (6-72)	34.7 $\pm$ 16.2 (10.7-90.3)	30.1 $\pm$ 17.4 (7.3-94.7)	16.7 $\pm$ 11.6 (6.3-69.7)	64.5 $\pm$ 15.5 (4.7-99.3)	46.8 $\pm$ 16.7 (12-86)	78.8 $\pm$ 5.3 (44-88)
<b>PWM (mm)</b>	73.4 $\pm$ 8.7 (46-90)	59.3 $\pm$ 14.5 (37-129)	73 $\pm$ 12.6 (43-178)	104.3 $\pm$ 64.5 (38-303)	70.3 $\pm$ 21.9 (38-147)	129.3 $\pm$ 28.8 (63-260)	94 $\pm$ 22 (45-220)	131.9 $\pm$ 11.8 (91-163)
<b>PDM (mm)</b>	1.1 $\pm$ 0.6 (0-2)	13.5 $\pm$ 7.7 (0-46)	24.2 $\pm$ 11.6 (5-79)	19.5 $\pm$ 11.3 (1-83)	9.7 $\pm$ 8 (0-46)	53.7 $\pm$ 14.9 (0-86)	36.9 $\pm$ 13.6 (5-73)	66 $\pm$ 4.8 (37-74)
<b>M (mm °C<sup>-1</sup>)</b>	17 $\pm$ 2.9 (9.1-24.9)	18.9 $\pm$ 4.5 (10.1-39.8)	29 $\pm$ 6.3 (16.7-61.8)	34.2 $\pm$ 18.7 (13.3-84.4)	19.8 $\pm$ 4 (13.4-36.7)	49.8 $\pm$ 9.8 (11.7-81)	43.1 $\pm$ 11.7 (18.3-98.6)	81.3 $\pm$ 12.1 (40.9-118)
<b>M1 (mm °C<sup>-1</sup>)</b>	2.4 $\pm$ 0.4 (1.3-3.5)	2.4 $\pm$ 0.6 (1.3-6)	3.6 $\pm$ 0.9 (1.5-8.9)	4.7 $\pm$ 2.6 (1.7-12.5)	2.9 $\pm$ 0.6 (1.8-5.4)	5.8 $\pm$ 1.3 (1.7-10.8)	5.3 $\pm$ 1.7 (1.8-13.4)	9.7 $\pm$ 1.6 (4.3-14.3)
<b>M2 (mm °C<sup>-1</sup>)</b>	3 $\pm$ 0.6 (1.5-4.6)	2 $\pm$ 0.7 (1-7.8)	3.3 $\pm$ 1.1 (1.1-8.9)	4.5 $\pm$ 2.8 (1.2-12.4)	2.5 $\pm$ 0.7 (1.4-6.6)	5.7 $\pm$ 1.3 (1.9-11.7)	5.1 $\pm$ 1.8 (1.5-12.9)	10 $\pm$ 1.9 (4.5-15.4)
<b>M3 (mm °C<sup>-1</sup>)</b>	0.7 $\pm$ 0.1 (0.4-1)	1.7 $\pm$ 0.4 (0.7-3.6)	2.8 $\pm$ 0.5 (1.6-5.6)	2.7 $\pm$ 1 (1.1-5.5)	1.6 $\pm$ 0.3 (1-3.3)	4.1 $\pm$ 0.8 (0.4-5.3)	4.1 $\pm$ 1 (1.8-10.1)	7.7 $\pm$ 1.3 (4.6-12.4)
<b>M4 (mm °C<sup>-1</sup>)</b>	0.2 $\pm$ 0 (0.1-0.4)	0.8 $\pm$ 0.4 (0.2-2.5)	1.2 $\pm$ 0.6 (0.4-3.2)	1.1 $\pm$ 0.6 (0.2-3.4)	0.5 $\pm$ 0.4 (0.2-2.3)	2.3 $\pm$ 0.5 (0.2-3.5)	1.8 $\pm$ 0.7 (0.4-4)	3.5 $\pm$ 0.4 (1.8-4.5)
<b>PET (mm)</b>	963.8 $\pm$ 44.5 (849-1095)	1068.5 $\pm$ 96 (817-1298)	974 $\pm$ 84.4 (747-1183)	1011.3 $\pm$ 131.5 (754-1340)	1129.6 $\pm$ 110.9 (827-1370)	839.1 $\pm$ 50.6 (748-1116)	860.9 $\pm$ 78.4 (592-1132)	640.8 $\pm$ 44.6 (522-831)
<b>PET1 (mm)</b>	56 $\pm$ 3.5 (47.7-65.7)	45.8 $\pm$ 5.5 (32.7-59.7)	38.4 $\pm$ 3.8 (28.3-49)	39.8 $\pm$ 5 (31-54.7)	46.1 $\pm$ 6.2 (33-57.3)	35.9 $\pm$ 4.8 (31-61)	32.4 $\pm$ 3 (22-46.7)	24.2 $\pm$ 1.8 (19.7-32.3)
<b>PET2 (mm)</b>	55.3 $\pm$ 3.7 (46-65.7)	47.5 $\pm$ 4.9 (35-62)	39.5 $\pm$ 3.3 (29.3-50.7)	41.8 $\pm$ 4.7 (32.7-56.3)	47.8 $\pm$ 5.4 (35.3-59)	38.4 $\pm$ 4.2 (32.7-61)	33.7 $\pm$ 3 (22-46.7)	24.3 $\pm$ 2.2 (18.7-31)
<b>PET3 (mm)</b>	95.9 $\pm$ 4.5 (83.7-109)	121.8 $\pm$ 8.9 (96.7-145.7)	112.1 $\pm$ 7.5 (89-132.3)	116.9 $\pm$ 13.7 (88.3-152)	129.8 $\pm$ 11.4 (98.3-154.3)	97.2 $\pm$ 4.8 (87-122)	100.2 $\pm$ 8.3 (69-128.3)	75.2 $\pm$ 5.4 (60.3-95.7)
<b>PET4 (mm)</b>	114.1 $\pm$ 3.6 (104.3-124.7)	141.1 $\pm$ 15.1 (108-178.7)	134.7 $\pm$ 14.6 (100-166.3)	138.6 $\pm$ 22.1 (92.3-184.7)	152.9 $\pm$ 18.3 (108.7-186.3)	108.2 $\pm$ 6.8 (92.3-148.7)	120.7 $\pm$ 12.9 (84.3-161)	90 $\pm$ 5.6 (75.3-121.7)

**Supplementary Table 2** Mean  $\pm$  standard deviation and range (minimum-maximum) of the climatic variables used to fit the climate-dependent MSDR models for broadleaf species.

	<i>Fagus sylvatica</i>	<i>Quercus faginea</i>	<i>Quercus ilex</i>	<i>Quercus petraea</i>	<i>Quercus pyrenaica</i>	<i>Quercus robur</i>	<i>Quercus suber</i>
<b>Plots</b>	1117	685	3609	201	1879	560	687
<b>T (°C)</b>	9.4 $\pm$ 1.3 (5.1-14)	11.2 $\pm$ 1.3 (8.2-17.6)	14 $\pm$ 2.2 (6.6-17.7)	9.5 $\pm$ 1.4 (6.5-14.6)	10.4 $\pm$ 1.5 (6-15.7)	12.1 $\pm$ 1.2 (6.1-14.5)	15.5 $\pm$ 1.3 (11.4-18)
<b>T1 (°C)</b>	7 $\pm$ 1.4 (2.9-12.4)	8 $\pm$ 1.2 (5.5-15)	10.5 $\pm$ 2.2 (3.4-15.2)	7 $\pm$ 1.4 (4-11.3)	7.4 $\pm$ 1.5 (3.2-12.2)	10 $\pm$ 1.4 (3.8-13.5)	12.7 $\pm$ 1.7 (7.8-16.2)
<b>T2 (°C)</b>	4 $\pm$ 1.4 (-0.3-9.6)	5.2 $\pm$ 1.2 (2.3-11.9)	7.7 $\pm$ 2.2 (0.1-12)	4 $\pm$ 1.4 (1-8.7)	4.7 $\pm$ 1.6 (0.1-9.7)	7.5 $\pm$ 1.4 (0.8-11)	9.8 $\pm$ 1.6 (5.3-13.1)
<b>T3 (°C)</b>	10.4 $\pm$ 1.5 (5.2-14.5)	12.6 $\pm$ 1.4 (9.1-18.4)	15.5 $\pm$ 2.2 (7.6-19.1)	10.6 $\pm$ 1.6 (6.8-16.1)	11.6 $\pm$ 1.6 (6.9-17.2)	12.9 $\pm$ 1.2 (6.2-15.8)	16.7 $\pm$ 1.1 (12.9-18.9)
<b>T4 (°C)</b>	16.2 $\pm$ 1.2 (12.5-19.4)	19 $\pm$ 1.7 (15.7-25)	22.4 $\pm$ 2.3 (14.5-25.7)	16.3 $\pm$ 1.5 (13.2-22.2)	17.9 $\pm$ 1.7 (13.3-24.3)	17.8 $\pm$ 1 (13.5-20.5)	23 $\pm$ 1.2 (18.3-25.9)
<b>MNT (°C)</b>	5.3 $\pm$ 1.2 (1.6-10.3)	5.8 $\pm$ 1.3 (2.7-11.9)	8.2 $\pm$ 2.1 (2-13.3)	5.2 $\pm$ 1.1 (2.7-9.4)	5.6 $\pm$ 1.5 (1.8-10.3)	7.8 $\pm$ 1.1 (2.5-11.2)	10.5 $\pm$ 1.6 (6.1-14.4)
<b>MNT1 (°C)</b>	3.4 $\pm$ 1.3 (0.1-8.8)	3.5 $\pm$ 1.3 (0.6-10.3)	5.8 $\pm$ 2.2 (0.4-11.4)	3.3 $\pm$ 1.1 (0.8-6.9)	3.4 $\pm$ 1.5 (-0.4-8)	6.4 $\pm$ 1.3 (0.9-10.5)	8.5 $\pm$ 1.8 (3.9-12.3)
<b>MNT2 (°C)</b>	-0.8 $\pm$ 1.4 (-4.9-5.9)	-1 $\pm$ 1.4 (-4.8-6.5)	0.8 $\pm$ 2.2 (-6.4-7.7)	-0.9 $\pm$ 1.3 (-4-3.9)	-1 $\pm$ 1.7 (-5.9-4.5)	2.6 $\pm$ 1.5 (-4-7.5)	4 $\pm$ 2.3 (-1.3-9.9)
<b>MNT3 (°C)</b>	5.7 $\pm$ 1.4 (0.9-10.7)	6.4 $\pm$ 1.4 (2.7-12.6)	8.6 $\pm$ 2 (1.3-13.9)	5.6 $\pm$ 1.3 (2.7-10.6)	6 $\pm$ 1.5 (1.8-10.7)	8 $\pm$ 1.2 (1.8-11.3)	10.9 $\pm$ 1.6 (6.3-15.2)
<b>MNT4 (°C)</b>	12.7 $\pm$ 1 (10.1-15.8)	14.5 $\pm$ 1.6 (11.5-20.3)	17.7 $\pm$ 2.2 (10.8-20.6)	12.7 $\pm$ 1.1 (10.7-17.3)	13.9 $\pm$ 1.6 (10.6-20)	14.2 $\pm$ 0.8 (10.9-16.2)	18.8 $\pm$ 1.1 (14.3-20.7)
<b>MXT (°C)</b>	13.5 $\pm$ 1.6 (8.6-18.3)	16.6 $\pm$ 1.6 (12.9-23.5)	19.8 $\pm$ 2.4 (11.2-24)	13.8 $\pm$ 1.9 (9.8-19.8)	15.3 $\pm$ 1.7 (9.8-21.3)	16.4 $\pm$ 1.4 (9.6-19.2)	20.6 $\pm$ 1.4 (16.6-24.2)
<b>MXT1 (°C)</b>	10.5 $\pm$ 1.6 (5.4-16)	12.5 $\pm$ 1.3 (9.7-19.7)	15.1 $\pm$ 2.3 (6.3-19.9)	10.6 $\pm$ 1.8 (6.9-16.3)	11.4 $\pm$ 1.6 (6.1-16.8)	13.7 $\pm$ 1.5 (6.4-16.8)	16.9 $\pm$ 1.7 (11.7-20.1)
<b>MXT2 (°C)</b>	8.7 $\pm$ 1.6 (4-14.3)	11.5 $\pm$ 1.4 (7.6-19)	14.7 $\pm$ 2.4 (6.4-19.1)	9 $\pm$ 1.8 (5.6-14.2)	10.4 $\pm$ 1.8 (5.1-16.3)	12.5 $\pm$ 1.6 (5.3-15.3)	15.6 $\pm$ 1.5 (11.8-19.4)
<b>MXT3 (°C)</b>	15.2 $\pm$ 1.7 (9.4-19.4)	18.9 $\pm$ 1.8 (14.5-25.6)	22.5 $\pm$ 2.5 (13.1-26.3)	15.5 $\pm$ 2.1 (10.8-21.6)	17.3 $\pm$ 1.9 (11.1-23.7)	17.9 $\pm$ 1.4 (10.7-21.5)	22.5 $\pm$ 1.5 (19.1-26.5)
<b>MXT4 (°C)</b>	19.8 $\pm$ 1.4 (14.8-23.4)	23.5 $\pm$ 2 (19.6-30.2)	27 $\pm$ 2.5 (18.1-31.2)	20 $\pm$ 2 (15.6-27.1)	21.9 $\pm$ 1.9 (16.1-28.6)	21.4 $\pm$ 1.2 (16.2-24.8)	27.2 $\pm$ 1.5 (22.3-31.1)
<b>MXTWM (°C)</b>	20.8 $\pm$ 1.4 (15.9-24.1)	24.7 $\pm$ 2.1 (20.7-31.7)	28.4 $\pm$ 2.5 (19.4-32.7)	21 $\pm$ 1.9 (16.7-28.3)	23 $\pm$ 2 (17.3-30)	22.2 $\pm$ 1.1 (17.5-25.5)	28.3 $\pm$ 1.5 (22.9-32.2)
<b>MNTCM (°C)</b>	-1.9 $\pm$ 1.3 (-5.7-5.2)	-2.7 $\pm$ 1.4 (-5.9-5.4)	-0.9 $\pm$ 2.2 (-7.2-6.6)	-2 $\pm$ 1.1 (-5.1-2.7)	-2.4 $\pm$ 1.7 (-7.5-4.1)	1.5 $\pm$ 1.6 (-5.1-6.8)	2.7 $\pm$ 2.5 (-3.2-8.9)
<b>TAR (°C)</b>	295.7 $\pm$ 1.5 (290.9-299.4)	300.4 $\pm$ 2.4 (294-306.5)	302.3 $\pm$ 2 (290.4-307.4)	296 $\pm$ 2 (292.2-300.5)	298.4 $\pm$ 2.2 (290.1-303.9)	293.6 $\pm$ 1.4 (288-298)	298.5 $\pm$ 3.1 (292.6-304.8)
<b>P (mm)</b>	1009.1 $\pm$ 122.6 (702-1396)	643.4 $\pm$ 173.2 (381-1041)	557.8 $\pm$ 142.3 (317-1567)	927 $\pm$ 155.5 (492-1405)	764.5 $\pm$ 244 (339-1763)	1371.7 $\pm$ 274.7 (753-1827)	683.8 $\pm$ 137.1 (359-1665)
<b>P1 (mm)</b>	101.2 $\pm$ 12.7 (68.7-161.3)	65.7 $\pm$ 17.9 (32-129)	67.9 $\pm$ 19.4 (30.7-199.7)	95.3 $\pm$ 21.6 (47.3-162.7)	86.8 $\pm$ 33.6 (37-218)	158 $\pm$ 40.8 (80.3-220.7)	89.3 $\pm$ 21.1 (40-205)
<b>P2 (mm)</b>	85.6 $\pm$ 12.6 (53.3-135)	52 $\pm$ 17.8 (20.3-119.7)	52.7 $\pm$ 18.5 (20.7-169.7)	77.1 $\pm$ 18.9 (39.3-138.3)	70.8 $\pm$ 30.3 (25.7-194.7)	139.6 $\pm$ 41.1 (64.3-216.7)	76.8 $\pm$ 27.7 (25.3-182.7)
<b>P3 (mm)</b>	90.5 $\pm$ 8.9 (67.7-117.7)	61.3 $\pm$ 14.4 (32.7-93.7)	46 $\pm$ 11.4 (30.3-99.7)	81.8 $\pm$ 9.9 (51-107)	65.1 $\pm$ 13.5 (30.7-114.7)	98.5 $\pm$ 10.7 (62.3-122.3)	43.6 $\pm$ 10.4 (29.7-108)
<b>P4 (mm)</b>	59.1 $\pm$ 9.5 (35-93.7)	35.5 $\pm$ 14.2 (7.7-76)	19.4 $\pm$ 13.2 (7.3-77)	54.7 $\pm$ 10.9 (26-85)	32.1 $\pm$ 11.1 (11-71.3)	61.1 $\pm$ 8.6 (39.7-102)	18.2 $\pm$ 16.6 (7-65)
<b>PWM (mm)</b>	109.1 $\pm$ 11.9 (84-174)	74.9 $\pm$ 18.4 (42-159)	78.5 $\pm$ 23.3 (38-216)	104.9 $\pm$ 20.1 (58-176)	98.4 $\pm$ 37.3 (40-251)	179.1 $\pm$ 51.8 (88-268)	105.7 $\pm$ 25.5 (44-240)
<b>PDM (mm)</b>	51.7 $\pm$ 8.3 (26-80)	28.7 $\pm$ 12.9 (1-59)	12 $\pm$ 10.9 (1-64)	45.1 $\pm$ 8.2 (19-71)	24.7 $\pm$ 10.5 (5-59)	43.5 $\pm$ 11.2 (22-87)	8.2 $\pm$ 10.8 (0-42)
<b>M (mm °C<sup>-1</sup>)</b>	52.1 $\pm$ 6.4 (40-82.7)	30.5 $\pm$ 8.8 (16.9-53.8)	23.5 $\pm$ 7.1 (12.5-65.8)	47.9 $\pm$ 9.4 (24.7-81.1)	37.6 $\pm$ 11.9 (14.1-80.2)	62.2 $\pm$ 12.1 (37.3-83.9)	26.9 $\pm$ 5.8 (14-72.9)
<b>M1 (mm °C<sup>-1</sup>)</b>	6.2 $\pm$ 0.8 (4.3-10.4)	3.7 $\pm$ 1 (1.8-7)	3.4 $\pm$ 1 (1.6-9.6)	5.8 $\pm$ 1.5 (2.9-11.4)	5.2 $\pm$ 1.9 (1.8-11.5)	8.1 $\pm$ 2.1 (4.3-11.8)	4 $\pm$ 0.9 (2-10)
<b>M2 (mm °C<sup>-1</sup>)</b>	6.2 $\pm$ 1 (3.7-11)	3.5 $\pm$ 1.1 (1.3-7.4)	3.1 $\pm$ 1.1 (1.3-9.9)	5.6 $\pm$ 1.5 (2.6-11.5)	4.9 $\pm$ 1.9 (1.5-11.8)	8 $\pm$ 2.3 (4-12.1)	3.9 $\pm$ 1.3 (1.4-10)
<b>M3 (mm °C<sup>-1</sup>)</b>	4.6 $\pm$ 0.5 (3.5-8.2)	2.8 $\pm$ 0.8 (1.2-4.8)	1.9 $\pm$ 0.6 (1.1-5.3)	4.2 $\pm$ 0.7 (2.5-6.2)	3.2 $\pm$ 0.8 (1.2-6.4)	4.5 $\pm$ 0.5 (2.5-7.1)	1.7 $\pm$ 0.5 (1.1-4.7)
<b>M4 (mm °C<sup>-1</sup>)</b>	2.3 $\pm$ 0.3 (1.4-3.7)	1.3 $\pm$ 0.5 (0.2-2.9)	0.6 $\pm$ 0.5 (0.2-3)	2.1 $\pm$ 0.4 (1-3.3)	1.2 $\pm$ 0.4 (0.4-2.6)	2.2 $\pm$ 0.3 (1.5-3.6)	0.6 $\pm$ 0.5 (0.2-2.3)
<b>PET (mm)</b>	848.4 $\pm$ 41.8 (645-937)	957.5 $\pm$ 93.7 (782-1332)	1132.9 $\pm$ 132.6 (719-1373)	850.8 $\pm$ 45.9 (727-952)	963.6 $\pm$ 80 (748-1215)	860.1 $\pm$ 47.6 (674-982)	1094.3 $\pm$ 125.3 (837-1379)
<b>PET1 (mm)</b>	32.7 $\pm$ 2.1 (24.3-38)	36.8 $\pm$ 3.9 (29.3-54)	44.8 $\pm$ 6.4 (27-57)	32.7 $\pm$ 2 (27.7-38)	35.9 $\pm$ 3.2 (28.3-48.3)	35.1 $\pm$ 1.7 (25.3-39.3)	47.8 $\pm$ 5.8 (34-58)
<b>PET2 (mm)</b>	34 $\pm$ 2.5 (24.3-41)	38.5 $\pm$ 4 (31.3-55.7)	46.6 $\pm$ 6 (28.3-59)	33.9 $\pm$ 2.4 (28.7-39)	37.5 $\pm$ 3.5 (29-49.7)	37.9 $\pm$ 2.2 (26-42.7)	49.4 $\pm$ 5.5 (36-59.7)
<b>PET3 (mm)</b>	99.1 $\pm$ 4.8 (76-109.7)	111.7 $\pm$ 10.1 (92.7-150.7)	130.1 $\pm$ 13.8 (85-154.7)	100 $\pm$ 5.2 (86-111)	112.1 $\pm$ 8.8 (87.7-140.7)	101 $\pm$ 5.9 (79.7-117)	123.5 $\pm$ 13.7 (99.3-155)
<b>PET4 (mm)</b>	117 $\pm$ 5.9 (90.3-129.7)	132.2 $\pm$ 14.3 (102.7-183.7)	156.2 $\pm$ 19 (99.3-187)	117 $\pm$ 6.9 (100-136)	135.7 $\pm$ 11.9 (96.3-172.3)	112.7 $\pm$ 7.7 (91-131)	144 $\pm$ 21.8 (109.3-187)

**Supplementary Table 3:** Species-specific coefficients, goodness of fits in terms of Akaike's Information Criterion (AIC) and pseudo-R<sup>2</sup> coefficient and SDI<sub>max</sub> estimations for the basic MSDR models fitted by linear quantile regression at the 95<sup>th</sup> and 99<sup>th</sup> quantiles.

Functional group	Species	tau	$\alpha_0$	$\beta_0$	SDI <sub>max</sub>	AIC	pseudo-R <sup>2</sup>	
Coniferous	<i>Pinus canariensis</i>	0.95	12.694 ***	-1.8631 ***	810	2514.7	0.3210	
		0.99	12.493 ***	-1.7431 ***	975	2710.5	0.3676	
	<i>Pinus halepensis</i>	0.95	11.971 ***	-1.8037 ***	476	12307.3	0.3151	
		0.99	11.738 ***	-1.6708 ***	578	12867.2	0.3665	
	<i>Pinus nigra</i>	0.95	12.516 ***	-1.7924 ***	851	4807.8	0.2971	
		0.99	12.892 ***	-1.8327 ***	1089	5484.2	0.2965	
	<i>Pinus pinaster</i>	0.95	13.213 ***	-1.9787 ***	938	10046.5	0.2744	
		0.99	13.065 ***	-1.8502 ***	1223	11170.9	0.2724	
	<i>Pinus pinea</i>	0.95	13.645 ***	-2.2517 ***	600	3002.5	0.3876	
		0.99	13.558 ***	-2.1227 ***	833	3599.1	0.3769	
	<i>Pinus radiata</i>	0.95	12.498 ***	-1.7161 ***	1069	1305.9	0.3624	
		0.99	13.233 ***	-1.8652 ***	1379	1571.5	0.3846	
	<i>Pinus sylvestris</i>	0.95	12.471 ***	-1.7118 ***	1055	7229.2	0.3550	
		0.99	12.736 ***	-1.7337 ***	1281	8307.9	0.3794	
	<i>Pinus uncinata</i>	0.95	13.332 ***	-2.0183 ***	930	539.7	0.4171	
		0.99	12.197 ***	-1.6159 ***	1092	572.0	0.4470	
	Broadleaf	<i>Fagus sylvatica</i>	0.95	13.283 ***	-2.0057 ***	922	1435.9	0.5188
			0.99	13.030 ***	-1.8756 ***	1089	1774.1	0.4990
<i>Quercus faginea</i>		0.95	12.307 ***	-1.8437 ***	585	1902.5	0.2057	
		0.99	12.224 ***	-1.6850 ***	898	2129.0	0.1389	
<i>Quercus ilex</i>		0.95	12.483 ***	-2.1209 ***	286	7723.4	0.5099	
		0.99	12.439 ***	-2.0294 ***	367	8503.5	0.4919	
<i>Quercus petraea</i>		0.95	12.077 ***	-1.6479 ***	874	387.8	0.3990	
		0.99	12.974 ***	-1.8351 ***	1173	479.4	0.3702	
<i>Quercus pyrenaica</i>		0.95	12.291 ***	-1.7838 ***	699	4565.1	0.2974	
		0.99	12.182 ***	-1.6603 ***	932	4848.3	0.3151	
<i>Quercus robur</i>		0.95	12.241 ***	-1.7466 ***	749	965.7	0.4265	
		0.99	12.066 ***	-1.6576 ***	837	1101.9	0.4214	
<i>Quercus suber</i>		0.95	12.530 ***	-1.9372 ***	542	1272.9	0.4834	
		0.99	12.319 ***	-1.8162 ***	647	1424.5	0.4731	

\*\*\* $p < 0.001$ ; \*\* $p < 0.01$ ; \* $p < 0.05$

**Supplementary Table 4.1:** Climate-dependent MSDR models for *Pinus canariensis* fitted at the 97.5<sup>th</sup> quantile arranged by AIC

model	$\alpha_0$	$\alpha_1$	$\beta_0$	$\beta_1$	AIC	pseudo-R <sup>2</sup>
T	107.072 ***	-16.757 ***	-1.6999 ***	-	2524.8	0.3642
T1	76.138 ***	-11.314 ***	-1.6712 ***	-	2554.2	0.3560
T2	81.878 ***	-12.343 ***	-1.6815 ***	-	2547.8	0.3578
T3	126.032 ***	-20.086 ***	-1.7406 ***	-	2502.1	0.3704
T4	206.414 ***	-34.143 ***	-1.8183 ***	-	2447.6	0.3850
MNT	96.203 ***	-14.857 ***	-1.7213 ***	-	2546.1	0.3583
MNT1	79.203 ***	-11.873 ***	-1.6778 ***	-	2559.4	0.3546
MNT2	68.779 ***	-10.070 ***	-1.6443 ***	-	2575.4	0.3501
MNT3	12.204 ***	-	3.2524 ***	-0.0175 ***	2542.7	0.3592
MNT4	159.366 ***	-25.941 ***	-1.7586 ***	-	2473.7	0.3781
MXT	111.833 ***	-17.545 ***	-1.7230 ***	-	2513.5	0.3673
MXT1	83.453 ***	-12.568 ***	-1.6919 ***	-	2555.3	0.3558
MXT2	96.515 ***	-14.864 ***	-1.7412 ***	-	2524.3	0.3643
MXT3	137.266 ***	-21.979 ***	-1.8149 ***	-	2478.6	0.3767
MXT4	192.808 ***	-31.680 ***	-1.8256 ***	-	2482.7	0.3756
MXTWM	231.904 ***	-38.519 ***	-1.8596 ***	-	2466.4	0.3800
MNTCM	261.436 **	-44.206 *	-12.8800 *	0.0398 *	2582.9	0.3486
TAR	-552.597 *	99.707 *	28.9155 *	-0.1061 *	2600.4	0.3436
P	13.161 ***	-	-2.6082 ***	0.0015 ***	2364.4	0.4067
P1	3.639 ***	2.448 ***	-2.0891 ***	-	2320.8	0.4178
P2	12.989 ***	-	-2.3961 ***	0.0075 ***	2420.9	0.3921
P3	12.954 ***	-	-2.2695 ***	0.0217 ***	2447.3	0.3851
P4	11.513 ***	0.739 ***	-1.8848 ***	-	2528.0	0.3633
PWM	4.176 ***	2.059 ***	-1.9567 ***	-	2347.4	0.4111
PDM	13.025 ***	0.071 **	-1.8108 ***	-0.1100 ***	2555.4	0.3563
M	10.028 ***	0.940 ***	-1.8486 ***	-	2435.8	0.3882
M1	11.738 ***	1.061 ***	-1.8500 ***	-	2431.5	0.3893
M2	12.005 ***	0.544 ***	-1.8100 ***	-	2488.1	0.3742
M3	12.646 ***	-	-2.0458 ***	0.3009 ***	2452.8	0.3836
M4	13.555 ***	0.576 ***	-1.8333 ***	-	2509.1	0.3685
PET	37.144 ***	-3.559 ***	-1.8398 ***	-	2488.2	0.3741
PET1	22.219 ***	-2.401 ***	-1.7990 ***	-	2496.4	0.3719
PET2	20.601 ***	-2.013 ***	-1.7907 ***	-	2499.1	0.3712
PET3	27.754 ***	-3.298 ***	-1.8447 ***	-	2504.4	0.3698
PET4	50.420 ***	-7.841 ***	-2.0254 ***	-	2479.2	0.3766

\*\*\* $p < 0.001$ ; \*\* $p < 0.01$ ; \* $p < 0.05$

**Supplementary Table 4.2:** Climate-dependent MSDR models for *Pinus halepensis* fitted at the 97.5<sup>th</sup> quantile arranged by AIC

model	$\alpha_0$	$\alpha_1$	$\beta_0$	$\beta_1$	AIC	pseudo-R <sup>2</sup>
T	262.676 **	-44.319 **	-14.2340 *	0.0435 *	12539.9	0.3435
T1	234.196 **	-39.372 **	-13.7142 **	0.0423 **	12598.1	0.3403
T2	236.144 **	-39.788 **	-13.6817 **	0.0426 **	12588.7	0.3408
T3	378.851 ***	-64.788 ***	-19.9687 ***	0.0632 ***	12491.2	0.3461
T4	367.474 ***	-62.531 ***	-18.0298 **	0.0552 **	12431.1	0.3493
MNT	223.305 ***	-37.485 ***	-13.5951 ***	0.0421 ***	12605.5	0.3399
MNT1	124.575 **	-20.006 *	-8.0578 **	0.0226 *	12617.0	0.3393
MNT2	-	-	-	-	-	-
MNT3	210.862 ***	-35.261 ***	-13.0329 ***	0.0400 **	12606.1	0.3399
MNT4	406.012 ***	-69.505 ***	-22.6423 ***	0.0720 ***	12525.2	0.3442
MXT	96.070 ***	-14.848 ***	-1.7000 ***	-	12406.5	0.3505
MXT1	49.417 ***	-6.642 ***	-1.7142 ***	-	12572.9	0.3416
MXT2	78.396 ***	-11.777 ***	-1.6945 ***	-	12448.3	0.3483
MXT3	96.948 ***	-14.977 ***	-1.7045 ***	-	12368.1	0.3526
MXT4	105.595 ***	-16.445 ***	-1.7171 ***	-	12383.7	0.3517
MXTWM	100.504 ***	-15.542 ***	-1.7134 ***	-	12394.4	0.3512
MNTCM	-	-	-	-	-	-
TAR	31.561 ***	-3.436 ***	-1.7624 ***	-	12562.0	0.3421
P	10.155 ***	0.280 ***	-1.7468 ***	-	12412.3	0.3502
P1	11.330 ***	0.155 ***	-1.7620 ***	-	12518.5	0.3445
P2	11.966 ***	-	-1.8124 ***	0.0010 ***	12530.6	0.3438
P3	10.919 ***	0.231 ***	-1.7162 ***	-	12497.5	0.3456
P4	12.249 ***	-0.117 *	-1.8022 ***	0.0022 **	12527.8	0.3441
PWM	8.722 ***	0.784 ***	-1.6057 ***	-0.0026 *	12401.9	0.3509
PDM	12.074 ***	-0.108 ***	-1.7813 ***	0.0043 ***	12510.0	0.3451
M	9.241 ***	0.886 ***	-1.5559 ***	-0.0095 **	12325.5	0.3549
M1	11.764 ***	0.216 ***	-1.7732 ***	-	12459.3	0.3477
M2	11.871 ***	0.157 ***	-1.7808 ***	-	12492.2	0.3459
M3	11.632 ***	0.227 ***	-1.7060 ***	-	12476.9	0.3467
M4	11.827 ***	-	-1.7531 ***	0.0295 ***	12533.5	0.3437
PET	28.421 ***	-2.389 *	-2.3564 ***	0.0006 *	12466.9	0.3474
PET1	13.155 ***	-0.378 ***	-1.6926 ***	-	12486.4	0.3462
PET2	13.676 ***	-0.505 ***	-1.6990 ***	-	12446.1	0.3484
PET3	24.672 ***	-2.670 **	-2.4245 ***	0.0056 *	12467.3	0.3474
PET4	25.074 ***	-2.671 ***	-2.5475 ***	0.0057 **	12498.1	0.3457

\*\*\* $p < 0.001$ ; \*\* $p < 0.01$ ; \* $p < 0.05$

**Supplementary Table 4.3:** Climate-dependent MSDR models for *Pinus nigra* fitted at the 97.5<sup>th</sup> quantile arranged by AIC

model	$\alpha_0$	$\alpha_1$	$\beta_0$	$\beta_1$	AIC	pseudo-R <sup>2</sup>
T	871.072 ***	-151.945 ***	-48.8820 ***	0.1657 ***	5074.5	0.3036
T1	-	-	-	-	-	-
T2	-	-	-	-	-	-
T3	815.154 ***	-141.912 ***	-44.8688 ***	0.1507 ***	5066.2	0.3048
T4	119.527 ***	-18.797 ***	-1.8521 ***	-	5063.2	0.3050
MNT	-	-	-	-	-	-
MNT1	568.796 ***	-98.980 ***	-35.8929 ***	0.1237 ***	5087.6	0.3016
MNT2	12.811 ***	-	-3.8799 ***	0.0075 **	5104.9	0.2987
MNT3	512.297 *	-88.755 *	-31.7062 *	0.1074 *	5089.2	0.3014
MNT4	748.493 **	-129.947 **	-40.9041 **	0.1358 **	5083.3	0.3023
MXT	154.667 ***	-24.995 ***	-1.9154 ***	-	5028.5	0.3102
MXT1	573.278 **	-99.152 **	-32.7777 **	0.1085 *	5085.6	0.3019
MXT2	13.019 ***	-	5.7005 ***	-0.0268 ***	5046.7	0.3075
MXT3	140.953 ***	-22.536 ***	-1.9324 ***	-	5010.9	0.3128
MXT4	104.610 ***	-16.094 **	-1.9119 ***	-	5045.9	0.3076
MXTWM	93.760 ***	-14.174 **	-1.9164 ***	-	5057.3	0.3059
MNTCM	12.800 ***	-	-4.1847 ***	0.0087 **	5100.9	0.2993
TAR	53.820 **	-7.171 *	-1.8746 ***	-	5067.2	0.3044
P	-	-	-	-	-	-
P1	11.568 ***	0.347 ***	-1.9117 ***	-	5056.4	0.3060
P2	11.821 ***	0.290 ***	-1.8973 ***	-	5047.8	0.3073
P3	-	-	-	-	-	-
P4	-	-	-	-	-	-
PWM	12.803 ***	-	-1.9221 ***	0.0010 *	5096.1	0.3001
PDM	-	-	-	-	-	-
M	11.963 ***	0.268 **	-1.8700 ***	-	5072.0	0.3037
M1	12.447 ***	0.334 ***	-1.8756 ***	-	5048.1	0.3072
M2	12.575 ***	0.282 ***	-1.8877 ***	-	5050.5	0.3069
M3	12.807 ***	-	-1.9221 ***	0.0246 *	5085.0	0.3017
M4	-	-	-	-	-	-
PET	-	-	-	-	-	-
PET1	-	-	-	-	-	-
PET2	-	-	-	-	-	-
PET3	-	-	-	-	-	-
PET4	-	-	-	-	-	-

\*\*\* $p < 0.001$ ; \*\* $p < 0.01$ ; \* $p < 0.05$

**Supplementary Table 4.4:** Climate-dependent MSDR models for *Pinus pinaster* fitted at the 97.5<sup>th</sup> quantile arranged by AIC

model	$\alpha_0$	$\alpha_1$	$\beta_0$	$\beta_1$	AIC	pseudo-R <sup>2</sup>
T	13.283 ***	-	3.6017 ***	-0.0195 ***	10357.7	0.2909
T1	70.461 ***	-10.167 ***	-1.9061 ***	-	10445.6	0.2838
T2	346.791 *	-59.217 *	-17.0639 *	0.0541 *	10449.5	0.2836
T3	13.324 ***	-	3.9110 ***	-0.0206 ***	10296.4	0.2958
T4	13.362 ***	-	2.8886 ***	-0.0167 ***	10360.4	0.2906
MNT	-	-	-	-	-	-
MNT1	329.208 ***	-56.126 **	-16.9772 **	0.0539 **	10523.2	0.2777
MNT2	333.907 ***	-57.140 ***	-17.7443 ***	0.0577 **	10522.1	0.2777
MNT3	74.361 ***	-10.863 ***	-1.9146 ***	-	10458.3	0.2828
MNT4	-435.827 **	79.282 **	26.8313 ***	-0.0998 ***	10430.3	0.2852
MXT	13.446 ***	-	4.1770 ***	-0.0213 ***	10229.0	0.3011
MXT1	99.279 ***	-15.226 ***	-1.9214 ***	-	10335.1	0.2927
MXT2	13.389 ***	-	3.3318 ***	-0.0187 ***	10317.1	0.2941
MXT3	13.365 ***	-	3.5759 ***	-0.0190 ***	10241.6	0.3001
MXT4	13.462 ***	-	2.6955 ***	-0.0159 ***	10307.5	0.2949
MXTWM	13.492 ***	-	2.3540 ***	-0.0147 ***	10329.3	0.2931
MNTCM	341.604 ***	-58.565 ***	-18.3189 ***	0.0601 ***	10531.9	0.2769
TAR	-440.516 ***	79.590 ***	23.5515 ***	-0.0852 ***	10489.8	0.2804
P	-	-	-	-	-	-
P1	-	-	-	-	-	-
P2	-	-	-	-	-	-
P3	8.636 ***	1.167 ***	-1.6924 ***	-0.0048 ***	10517.0	0.2782
P4	11.446 ***	0.556 ***	-1.8094 ***	-0.0048 ***	10492.2	0.2802
PWM	-	-	-	-	-	-
PDM	13.124 ***	0.106 ***	-2.0045 ***	-	10513.0	0.2783
M	11.641 ***	0.489 **	-1.8491 ***	-0.0035 **	10542.3	0.2761
M1	-	-	-	-	-	-
M2	-	-	-	-	-	-
M3	-	-	-	-	-	-
M4	12.712 ***	0.866 **	-1.8330 ***	-0.0752 **	10483.1	0.2809
PET	13.329 ***	0.461 ***	-1.8409 ***	-0.1135 ***	10475.7	0.2815
PET1	13.246 ***	-	-1.8523 ***	-0.0001 *	10569.4	0.2737
PET2	13.306 ***	-	-1.7219 ***	-0.0062 ***	10432.2	0.2849
PET3	13.340 ***	-	-1.7265 ***	-0.0061 ***	10430.2	0.2850
PET4	-27.039 ***	8.433 ***	0.7719 *	-0.0228 ***	10403.1	0.2874

\*\*\* $p < 0.001$ ; \*\* $p < 0.01$ ; \* $p < 0.05$

**Supplementary Table 4.5:** Climate-dependent MSDR models for *Pinus pinea* fitted at the 97.5<sup>th</sup> quantile arranged by AIC

model	$\alpha_0$	$\alpha_1$	$\beta_0$	$\beta_1$	AIC	pseudo-R <sup>2</sup>
T	-	-	-	-	-	-
T1	-	-	-	-	-	-
T2	13.505 ***	-	-4.4234 ***	0.0080 *	3257.7	0.3921
T3	-	-	-	-	-	-
T4	-	-	-	-	-	-
MNT	-	-	-	-	-	-
MNT1	13.650 ***	-	-4.5010 ***	0.0082 *	3250.2	0.3938
MNT2	13.763 ***	-	-4.7594 ***	0.0091 ***	3235.8	0.3970
MNT3	13.565 ***	-	-5.1013 ***	0.0103 **	3245.7	0.3948
MNT4	-	-	-	-	-	-
MXT	-	-	-	-	-	-
MXT1	-	-	-	-	-	-
MXT2	-	-	-	-	-	-
MXT3	-	-	-	-	-	-
MXT4	-	-	-	-	-	-
MXTWM	-	-	-	-	-	-
MNTCM	-29.493 *	7.684 **	-2.2089 ***	-	3228.5	0.3986
TAR	77.368 **	-11.127 *	-2.2790 ***	-	3213.2	0.4020
P	13.213 ***	-	-2.2271 ***	0.0003 **	3210.7	0.4026
P1	-	-	-	-	-	-
P2	-	-	-	-	-	-
P3	13.465 ***	-	-2.4048 ***	0.0063 ***	3226.9	0.3990
P4	15.072 ***	-0.460 *	-2.4379 ***	0.0093 ***	3139.5	0.4185
PWM	-	-	-	-	-	-
PDM	14.023 ***	-	-2.3647 ***	0.0039 *	3228.1	0.3987
M	13.304 ***	-	-2.2518 ***	0.0077 *	3216.7	0.4013
M1	-	-	-	-	-	-
M2	-	-	-	-	-	-
M3	13.649 ***	-	-2.3483 ***	0.0875 *	3249.1	0.3940
M4	13.531 ***	-0.467 **	-2.4556 ***	0.2919 ***	3144.0	0.4176
PET	20.341 ***	-0.887 *	-2.3588 ***	-	3232.4	0.3978
PET1	-	-	-	-	-	-
PET2	-	-	-	-	-	-
PET3	14.074 ***	-	-2.0350 ***	-0.0024 *	3238.5	0.3964
PET4	17.595 ***	-0.713 **	-2.3301 ***	-	3226.0	0.3992

\*\*\* $p < 0.001$ ; \*\* $p < 0.01$ ; \* $p < 0.05$

**Supplementary Table 4.6:** Climate-dependent MSDR models for *Pinus radiata* fitted at the 97.5<sup>th</sup> quantile arranged by AIC

model	$\alpha_0$	$\alpha_1$	$\beta_0$	$\beta_1$	AIC	pseudo-R <sup>2</sup>
T	-	-	-	-	-	-
T1	-	-	-	-	-	-
T2	-	-	-	-	-	-
T3	-	-	-	-	-	-
T4	-	-	-	-	-	-
MNT	-	-	-	-	-	-
MNT1	-	-	-	-	-	-
MNT2	-	-	-	-	-	-
MNT3	-	-	-	-	-	-
MNT4	-	-	-	-	-	-
MXT	-	-	-	-	-	-
MXT1	-	-	-	-	-	-
MXT2	-	-	-	-	-	-
MXT3	-	-	-	-	-	-
MXT4	-	-	-	-	-	-
MXTWM	-	-	-	-	-	-
MNTCM	-	-	-	-	-	-
TAR	-	-	-	-	-	-
P	-	-	-	-	-	-
P1	-	-	-	-	-	-
P2	-	-	-	-	-	-
P3	-	-	-	-	-	-
P4	-	-	-	-	-	-
PWM	-	-	-	-	-	-
PDM	-	-	-	-	-	-
M	-	-	-	-	-	-
M1	-	-	-	-	-	-
M2	-	-	-	-	-	-
M3	-	-	-	-	-	-
M4	-	-	-	-	-	-
PET	-	-	-	-	-	-
PET1	6.920 **	1.675 *	-1.3894 ***	-0.0119 **	1421.2	0.3778
PET2	-	-	-	-	-	-
PET3	110.968 ***	-21.507 ***	-8.0490 ***	0.0652 ***	1402.4	0.3845
PET4	88.959 ***	-16.269 **	-6.5496 ***	0.0441 **	1409.2	0.3821

\*\*\* $p < 0.001$ ; \*\* $p < 0.01$ ; \* $p < 0.05$

**Supplementary Table 4.7:** Climate-dependent MSDR models for *Pinus sylvestris* fitted at the 97.5<sup>th</sup> quantile arranged by AIC

model	$\alpha_0$	$\alpha_1$	$\beta_0$	$\beta_1$	AIC	pseudo-R <sup>2</sup>
T	-	-	-	-	-	-
T1	-	-	-	-	-	-
T2	-	-	-	-	-	-
T3	-	-	-	-	-	-
T4	55.518 **	-7.547 *	-1.7711 ***	-	7697.6	0.3698
MNT	-	-	-	-	-	-
MNT1	-	-	-	-	-	-
MNT2	322.444 *	-55.329 *	-21.8988 *	0.0746 *	7673.7	0.3718
MNT3	-	-	-	-	-	-
MNT4	-	-	-	-	-	-
MXT	65.896 ***	-9.391 ***	-1.7774 ***	-	7664.1	0.3724
MXT1	54.869 ***	-7.463 ***	-1.7703 ***	-	7679.3	0.3712
MXT2	41.879 **	-5.164 *	-1.7745 ***	-	7696.3	0.3699
MXT3	58.945 ***	-8.154 ***	-1.7767 ***	-	7653.0	0.3732
MXT4	71.686 ***	-10.376 ***	-1.7699 ***	-	7643.9	0.3739
MXTWM	74.540 ***	-10.872 ***	-1.7675 ***	-	7637.6	0.3744
MNTCM	617.791 ***	-108.147 ***	-40.0934 ***	0.1425 ***	7630.1	0.3751
TAR	66.470 ***	-9.442 ***	-1.7478 ***	-	7594.7	0.3777
P	-	-	-	-	-	-
P1	-	-	-	-	-	-
P2	12.110 ***	0.107 **	-1.7104 ***	-	7675.6	0.3715
P3	-	-	-	-	-	-
P4	-	-	-	-	-	-
PWM	-	-	-	-	-	-
PDM	-	-	-	-	-	-
M	12.579 ***	-	-1.7462 ***	0.0007 *	7704.4	0.3693
M1	12.390 ***	0.107 **	-1.7119 ***	-	7684.3	0.3708
M2	12.375 ***	0.115 ***	-1.7107 ***	-	7670.7	0.3719
M3	-	-	-	-	-	-
M4	-	-	-	-	-	-
PET	-	-	-	-	-	-
PET1	12.675 ***	-	-1.6454 ***	-0.0031 *	7709.1	0.3689
PET2	-	-	-	-	-	-
PET3	-	-	-	-	-	-
PET4	-	-	-	-	-	-

\*\*\* $p < 0.001$ ; \*\* $p < 0.01$ ; \* $p < 0.05$

**Supplementary Table 4.8:** Climate-dependent MSDR models for *Pinus uncinata* fitted at the 97.5<sup>th</sup> quantile arranged by AIC

model	$\alpha_0$	$\alpha_1$	$\beta_0$	$\beta_1$	AIC	pseudo-R <sup>2</sup>
T	65.799 ***	-9.413 **	-1.8310 ***	-	541.6	0.4536
T1	72.583 **	-10.637 *	-1.8259 ***	-	542.5	0.4530
T2	62.186 **	-8.808 *	-1.8206 ***	-	550.6	0.4472
T3	-	-	-	-	-	-
T4	-	-	-	-	-	-
MNT	-	-	-	-	-	-
MNT1	-	-	-	-	-	-
MNT2	-	-	-	-	-	-
MNT3	65.683 **	-9.395 *	-1.8730 ***	-	544.1	0.4518
MNT4	73.860 **	-10.813 *	-1.8292 ***	-	548.7	0.4486
MXT	-	-	-	-	-	-
MXT1	74.959 ***	-11.002 **	-1.9032 ***	-	539.0	0.4555
MXT2	55.316 **	-7.575 *	-1.7969 ***	-	542.7	0.4528
MXT3	52.975 ***	-7.087 **	-1.8875 ***	-	540.9	0.4541
MXT4	60.606 ***	-8.384 ***	-1.9346 ***	-	539.5	0.4551
MXTWM	56.182 **	-7.606 *	-1.9176 ***	-	540.0	0.4547
MNTCM	-	-	-	-	-	-
TAR	57.065 **	-7.756 *	-1.8802 ***	-	546.6	0.4500
P	9.699 ***	0.451 *	-1.8620 ***	-	542.5	0.4530
P1	11.168 ***	0.363 *	-1.8635 ***	-	540.0	0.4548
P2	11.386 ***	0.364 ***	-1.9112 ***	-	538.1	0.4561
P3	-	-	-	-	-	-
P4	-	-	-	-	-	-
PWM	-	-	-	-	-	-
PDM	-	-	-	-	-	-
M	11.993 ***	0.228 *	-1.8876 ***	-	541.0	0.4541
M1	12.856 ***	-	-1.9196 ***	0.0077 **	539.0	0.4555
M2	12.364 ***	0.203 **	-1.8344 ***	-	540.6	0.4543
M3	-	-	-	-	-	-
M4	-	-	-	-	-	-
PET	12.899 ***	-	-1.6288 ***	-0.0004 **	535.6	0.4578
PET1	12.896 ***	-	-1.6636 ***	-0.0082 *	538.6	0.4558
PET2	12.908 ***	-	-1.6784 ***	-0.0077 **	536.7	0.4571
PET3	12.918 ***	-	-1.6378 ***	-0.0031 **	534.6	0.4586
PET4	16.777 ***	-0.838 ***	-1.8979 ***	-	535.5	0.4580

\*\*\* $p < 0.001$ ; \*\* $p < 0.01$ ; \* $p < 0.05$

**Supplementary Table 4.9:** Climate-dependent MSDR models for *Fagus sylvatica* fitted at the 97.5<sup>th</sup> quantile arranged by AIC

model	$\alpha_0$	$\alpha_1$	$\beta_0$	$\beta_1$	AIC	pseudo-R <sup>2</sup>
T	84.978 ***	-12.783 ***	-1.8450 ***	-	1520.2	0.5264
T1	69.028 ***	-9.970 **	-1.8495 ***	-	1528.6	0.5246
T2	71.240 ***	-10.382 **	-1.8500 ***	-	1524.0	0.5255
T3	12.813 ***	-	2.0872 *	-0.0138 ***	1510.2	0.5285
T4	12.771 ***	-	3.2512 ***	-0.0176 ***	1521.3	0.5261
MNT	72.193 ***	-10.536 ***	-1.8614 ***	-	1533.1	0.5236
MNT1	61.002 ***	-8.555 ***	-1.8669 ***	-	1537.9	0.5226
MNT2	60.650 ***	-8.525 **	-1.8516 ***	-	1542.0	0.5217
MNT3	76.863 ***	-11.370 ***	-1.8514 ***	-	1531.2	0.5240
MNT4	100.456 ***	-15.481 **	-1.8687 ***	-	1529.6	0.5244
MXT	84.592 ***	-12.675 ***	-1.8615 ***	-	1515.0	0.5275
MXT1	70.247 ***	-10.155 ***	-1.8648 ***	-	1523.2	0.5257
MXT2	75.624 ***	-11.138 ***	-1.8360 ***	-	1512.2	0.5281
MXT3	12.870 ***	-	2.0880 ***	-0.0137 ***	1507.5	0.5290
MXT4	12.966 ***	-	1.9497 ***	-0.0131 ***	1523.2	0.5257
MXTWM	12.952 ***	-	2.4228 ***	-0.0147 ***	1528.7	0.5245
MNTCM	49.285 **	-6.485 *	-1.8831 ***	-	1551.5	0.5197
TAR	-	-	-	-	-	-
P	-	-	-	-	-	-
P1	13.387 ***	-	-2.1378 ***	0.0012 ***	1564.8	0.5168
P2	-	-	-	-	-	-
P3	-	-	-	-	-	-
P4	-	-	-	-	-	-
PWM	11.163 ***	0.469 ***	-2.0059 ***	-	1563.5	0.5171
PDM	-	-	-	-	-	-
M	13.279 ***	-	-2.1438 ***	0.0031 ***	1529.2	0.5244
M1	12.133 ***	0.671 ***	-2.0013 ***	-	1514.9	0.5275
M2	12.406 ***	0.450 ***	-1.9686 ***	-	1528.0	0.5247
M3	13.290 ***	-	-2.1362 ***	0.0326 **	1539.8	0.5222
M4	13.488 ***	-	-2.1392 ***	0.0421 *	1563.7	0.5171
PET	13.036 ***	-	-1.5861 ***	-0.0004 ***	1533.2	0.5236
PET1	12.911 ***	-	-1.5935 ***	-0.0085 ***	1514.5	0.5276
PET2	12.851 ***	-	-1.6180 ***	-0.0068 **	1517.0	0.5270
PET3	13.018 ***	-	-1.6126 ***	-0.0029 ***	1545.1	0.5210
PET4	-	-	-	-	-	-

\*\*\* $p < 0.001$ ; \*\* $p < 0.01$ ; \* $p < 0.05$

**Supplementary Table 4.10:** Climate-dependent MSDR models for *Quercus faginea* fitted at the 97.5<sup>th</sup> quantile arranged by AIC

model	$\alpha_0$	$\alpha_1$	$\beta_0$	$\beta_1$	AIC	pseudo-R <sup>2</sup>
T	12.436 ***	-	8.7757 *	-0.0374 **	1970.3	0.2019
T1	-	-	-	-	-	-
T2	-	-	-	-	-	-
T3	233.156 ***	-38.984 **	-1.9505 ***	-	1960.8	0.2073
T4	271.627 ***	-45.750 ***	-1.6856 ***	-	1910.6	0.2359
MNT	-	-	-	-	-	-
MNT1	-1047.998 **	188.507 **	63.4382 **	-0.2352 **	1991.1	0.1908
MNT2	-	-	-	-	-	-
MNT3	-	-	-	-	-	-
MNT4	275.616 ***	-46.563 ***	-1.7134 ***	-	1934.1	0.2227
MXT	204.087 **	-33.789 **	-1.9014 ***	-	1944.0	0.2170
MXT3	12.416 ***	-	7.8794 *	-0.0340 *	1977.7	0.1975
MXT4	190.412 **	-31.459 **	-1.9219 ***	-	1968.4	0.2029
MXTWM	202.428 **	-33.429 **	-1.9483 ***	-	1934.4	0.2225
MNTCM	254.074 ***	-42.519 ***	-1.7485 ***	-	1899.6	0.2420
TAR	247.037 ***	-41.233 ***	-1.7874 ***	-	1883.7	0.2508
P	-	-	-	-	-	-
P1	12.606 ***	-	12.9044 ***	-0.0495 ***	1886.9	0.249
P2	7.655 ***	0.703 ***	-1.7754 ***	-	1933.3	0.2231
P3	9.939 ***	0.568 **	-1.8101 ***	-	1959.9	0.2079
P4	9.747 ***	0.686 ***	-1.8566 ***	-	1940.6	0.2190
PWM	8.949 ***	0.800 ***	-1.7900 ***	-	1930.8	0.2245
PDM	10.242 ***	0.542 ***	-1.7612 ***	-	1952.0	0.2124
M	8.663 ***	0.813 ***	-1.7536 ***	-	1960.1	0.2078
M1	13.080 ***	-0.249 *	-2.0875 ***	0.0095 ***	1928.2	0.2271
M2	9.667 ***	0.812 ***	-1.8657 ***	-	1915.9	0.2329
M3	11.463 ***	0.645 *	-1.8078 ***	-	1948.8	0.2142
M4	11.662 ***	0.691 ***	-1.8910 ***	-	1922.7	0.2291
PET	11.375 ***	0.838 ***	-1.7905 ***	-	1919.0	0.2312
PET1	12.083 ***	0.516 ***	-1.7726 ***	-	1943.5	0.2173
PET2	12.066 ***	-	-0.8581 ***	-0.0009 ***	1944.3	0.2169
PET3	20.420 ***	-2.270 ***	-1.8082 ***	-	1957.5	0.2093
PET4	20.828 ***	-2.343 ***	-1.8209 ***	-	1949.2	0.2140

\*\*\* $p < 0.001$ ; \*\* $p < 0.01$ ; \* $p < 0.05$

**Supplementary Table 4.11:** Climate-dependent MSDR models for *Quercus ilex* fitted at the 97.5<sup>th</sup> quantile arranged by AIC

model	$\alpha_0$	$\alpha_1$	$\beta_0$	$\beta_1$	AIC	pseudo-R <sup>2</sup>
T	11.966 ***	-	5.4244 ***	-0.0256 ***	7614.5	0.5350
T1	11.99 ***	-	4.3763 ***	-0.0223 ***	7761.6	0.5254
T2	11.959 ***	-	4.5974 ***	-0.0232 ***	7718.4	0.5283
T3	-203.752 **	38.076 **	18.6551 ***	-0.0713 ***	7548.9	0.5393
T4	12.000 ***	-	5.1724 ***	-0.0241 ***	7517.9	0.5412
MNT	12.059 ***	-	4.3424 ***	-0.0224 ***	7785.8	0.5238
MNT1	12.064 ***	-	3.5385 ***	-0.0197 ***	7880.2	0.5176
MNT2	12.221 ***	-	2.3123 ***	-0.0158 ***	7950.2	0.5129
MNT3	-183.104 *	34.619 *	15.2413 **	-0.0612 ***	7786.2	0.5239
MNT4	-171.905 **	32.405 **	16.2231 ***	-0.0624 ***	7576.3	0.5376
MXT	11.882 ***	-	5.3381 ***	-0.0248 ***	7523.0	0.5409
MXT1	11.963 ***	-	4.5508 ***	-0.0225 ***	7671.1	0.5313
MXT2	127.035 ***	-20.350 ***	-1.8931 ***	-	7568.2	0.5380
MXT3	11.899 ***	-	5.0064 ***	-0.0234 ***	7474.1	0.5440
MXT4	11.963 ***	-	5.0802 ***	-0.0234 ***	7491.1	0.5429
MXTWM	11.969 ***	-	4.7651 ***	-0.0223 ***	7484.2	0.5433
MNTCM	59.321 ***	-8.377 ***	-2.0487 ***	-	8017.5	0.5083
TAR	12.342 ***	-	2.9730 ***	-0.0166 ***	7749.4	0.5262
P	12.474 ***	-	-2.2131 ***	0.0002 ***	7877.8	0.5177
P1	-	-	-	-	-	-
P2	-	-	-	-	-	-
P3	10.088 ***	0.559 ***	-2.0213 ***	-	7640.1	0.5333
P4	11.433 ***	0.220 ***	-1.9687 ***	-	7634.6	0.5337
PWM	-	-	-	-	-	-
PDM	12.004 ***	-	-1.9947 ***	0.0037 ***	7635.8	0.5336
M	12.379 ***	-	-2.1959 ***	0.0054 ***	7747.0	0.5264
M1	12.342 ***	0.267 ***	-2.1479 ***	-	8013.3	0.5086
M2	12.387 ***	0.220 ***	-2.1347 ***	-	7997.2	0.5097
M3	11.702 ***	0.541 ***	-1.9684 ***	-	7549.0	0.5392
M4	12.139 ***	0.215 ***	-1.9555 ***	-	7588.7	0.5367
PET	11.773 ***	-	-1.4050 ***	-0.0004 ***	7449.7	0.5455
PET1	11.881 ***	-	-1.5566 ***	-0.0078 ***	7564.1	0.5382
PET2	11.865 ***	-	-1.5025 ***	-0.0087 ***	7491.1	0.5429
PET3	11.777 ***	-	-1.3094 ***	-0.0044 ***	7398.6	0.5487
PET4	11.909 ***	-	-1.5462 ***	-0.0024 ***	7510.4	0.5417

\*\*\* $p < 0.001$ ; \*\* $p < 0.01$ ; \* $p < 0.05$

**Supplementary Table 4.12:** Climate-dependent MSDR models for *Quercus petraea* fitted at the 97.5<sup>th</sup> quantile arranged by AIC

model	$\alpha_0$	$\alpha_1$	$\beta_0$	$\beta_1$	AIC	pseudo-R <sup>2</sup>
T	12.404 ***	-	11.6926 ***	-0.0475 ***	369.3	0.4779
T1	12.335 ***	-	12.6721 ***	-0.0513 ***	378.7	0.4656
T2	12.338 ***	-	10.9878 ***	-0.0458 ***	380.4	0.4633
T3	12.429 ***	-	9.9918 ***	-0.0414 ***	364.9	0.4836
T4	12.674 ***	-	11.0925 ***	-0.0446 ***	361.6	0.4878
MNT	-1169.241 ***	209.898 ***	82.0857 ***	-0.3009 ***	385.4	0.4593
MNT1	12.140 ***	-	12.0032 **	-0.0493 **	397.8	0.4396
MNT2	12.380 ***	-	11.4710 ***	-0.0484 ***	411.1	0.4207
MNT3	12.308 ***	-	10.6062 ***	-0.0441 ***	388.8	0.4519
MNT4	12.689 ***	-	13.1134 ***	-0.0523 ***	371.1	0.4756
MXT	-489.861 ***	88.759 ***	36.5003 ***	-0.1334 ***	357.6	0.4954
MXT1	12.623 ***	-	10.8801 **	-0.0447 ***	369.6	0.4775
MXT2	-348.430 *	63.966 *	28.0916 ***	-0.1058 ***	363.2	0.4883
MXT3	12.615 ***	-	7.5139 ***	-0.0323 ***	360.0	0.4899
MXT4	12.593 ***	-	9.0312 ***	-0.0370 ***	358.5	0.4917
MXTWM	12.382 ***	-	8.8624 ***	-0.0360 ***	360.8	0.4889
MNTCM	12.602 ***	-	10.6650 ***	-0.0459 ***	429.1	0.3942
TAR	157.524 **	-25.493 **	-1.7459 ***	-	381.0	0.4625
P	-	-	-	-	-	-
P1	-	-	-	-	-	-
P2	4.285 *	1.879 ***	-1.2898 ***	-0.0054 ***	419.1	0.4120
P3	-	-	-	-	-	-
P4	12.565 ***	-	-1.3686 ***	-0.0075 ***	398.0	0.4392
PWM	32.910 ***	-4.432 **	-2.9490 ***	0.0119 **	419.5	0.4114
PDM	12.808 ***	-	-1.4380 ***	-0.0088 ***	415.9	0.4137
M	-	-	-	-	-	-
M1	10.500 ***	0.818 ***	-1.5610 ***	-	416.1	0.4135
M2	10.786 ***	0.818 **	-1.6339 ***	-	410.9	0.4209
M3	23.887 ***	-8.481 ***	-4.2699 ***	0.6577 ***	398.5	0.4414
M4	12.167 ***	-	-1.3617 ***	-0.1387 ***	427.3	0.3969
PET	12.289 ***	-	-0.8605 *	-0.0009 *	421.7	0.4053
PET1	12.013 ***	-	-0.4393 *	-0.0345 ***	401.2	0.4349
PET2	12.283 ***	-	-0.6573 **	-0.0298 ***	385.2	0.4568
PET3	22.509 ***	-2.189 *	-1.7088 ***	-	421.0	0.4062
PET4	11.831 ***	-	-2.1149 ***	0.0049 **	431.4	0.3907

\*\*\* $p < 0.001$ ; \*\* $p < 0.01$ ; \* $p < 0.05$

**Supplementary Table 4.13:** Climate-dependent MSDR models for *Quercus pyrenaica* fitted at the 97.5<sup>th</sup> quantile arranged by AIC

model	$\alpha_0$	$\alpha_1$	$\beta_0$	$\beta_1$	AIC	pseudo-R <sup>2</sup>
T	-287.444 **	53.090 **	23.9132 ***	-0.0906 ***	4589.0	0.3207
T1	-320.175 **	58.994 ***	25.2750 ***	-0.0964 ***	4636.4	0.3121
T2	-	-	-	-	-	-
T3	-296.017 **	54.575 **	24.1656 ***	-0.0912 ***	4593.5	0.3199
T4	-187.581 *	35.255 *	17.9460 ***	-0.0679 ***	4537.2	0.330
MNT	-328.016 **	60.450 ***	25.9570 ***	-0.0994 ***	4641.4	0.3112
MNT1	12.287 ***	-	3.0745 *	-0.0174 ***	4669.0	0.3057
MNT2	62.927 **	-9.041 *	-1.7177 ***	-	4702.2	0.2996
MNT3	12.300 ***	-	3.0244 *	-0.0171 ***	4676.4	0.3044
MNT4	12.312 ***	-	7.1163 ***	-0.0309 ***	4566.5	0.3244
MXT	-255.561 *	47.321 *	20.7678 **	-0.0783 **	4578.4	0.3226
MXT1	12.178 ***	-	3.1939 ***	-0.0172 ***	4640.7	0.3110
MXT2	12.309 ***	-	3.8858 ***	-0.0199 ***	4616.6	0.3154
MXT3	-310.973 *	57.023 *	24.1039 **	-0.0892 ***	4577.6	0.3228
MXT4	12.328 ***	-	5.5596 ***	-0.0248 ***	4578.1	0.3223
MXTWM	12.335 ***	-	5.6320 ***	-0.0250 ***	4570.0	0.3238
MNTCM	-	-	-	-	-	-
TAR	64.485 ***	-9.175 ***	-1.7080 ***	-	4679.1	0.3039
P	-	-	-	-	-	-
P1	-	-	-	-	-	-
P2	-	-	-	-	-	-
P3	10.821 ***	0.320 *	-1.6870 ***	-	4686.2	0.3026
P4	11.172 ***	0.297 ***	-1.7067 ***	-	4629.3	0.3130
PWM	-	-	-	-	-	-
PDM	11.570 ***	0.234 ***	-1.7462 ***	-	4608.1	0.3169
M	9.809 ***	0.677 **	-1.5369 ***	-0.0047 *	4697.6	0.3008
M1	-	-	-	-	-	-
M2	-	-	-	-	-	-
M3	11.766 ***	0.371 ***	-1.7009 ***	-	4647.6	0.3097
M4	12.156 ***	0.275 ***	-1.7087 ***	-	4617.2	0.3153
PET	12.270 ***	-	-1.2285 ***	-0.0005 ***	4584.9	0.3211
PET1	12.222 ***	-	-1.2564 ***	-0.0130 ***	4599.0	0.3186
PET2	12.364 ***	-	-1.3735 ***	-0.0105 ***	4593.1	0.3196
PET3	12.306 ***	-	-1.1779 ***	-0.0052 ***	4584.0	0.3213
PET4	12.269 ***	-	-1.2806 ***	-0.0034 ***	4596.3	0.3190

\*\*\* $p < 0.001$ ; \*\* $p < 0.01$ ; \* $p < 0.05$

**Supplementary Table 4.14:** Climate-dependent MSDR models for *Quercus robur* fitted at the 97.5<sup>th</sup> quantile arranged by AIC

model	$\alpha_0$	$\alpha_1$	$\beta_0$	$\beta_1$	AIC	pseudo-R <sup>2</sup>
T	-658.148 *	118.548 *	41.3317 *	-0.1508 *	1001.0	0.4497
T1	-602.202 ***	108.830 ***	37.3468 ***	-0.1381 ***	996.3	0.4520
T2	76.724 ***	-11.442 ***	-1.7353 ***	-	1002.7	0.4479
T3	92.442 ***	-14.184 ***	-1.7317 ***	-	1007.5	0.4455
T4	81.830 ***	-12.287 ***	-1.7053 ***	-	1011.0	0.4437
MNT	-820.659 ***	147.740 ***	51.1787 ***	-0.1885 ***	981.1	0.4594
MNT1	-624.820 **	113.080 **	39.0364 **	-0.1458 **	993.6	0.4533
MNT2	-605.574 ***	109.939 ***	37.8316 ***	-0.1435 ***	985.5	0.4572
MNT3	-795.789 ***	143.317 ***	49.1578 ***	-0.1812 ***	974.7	0.4624
MNT4	-1112.201 ***	198.611 ***	70.2864 ***	-0.2505 ***	989.2	0.4554
MXT	63.703 ***	-9.108 ***	-1.6903 ***	-	1011.8	0.4433
MXT1	74.444 ***	-11.004 ***	-1.7205 ***	-	1004.9	0.4468
MXT2	61.685 ***	-8.777 ***	-1.6824 ***	-	1011.1	0.4437
MXT3	-	-	-	-	-	-
MXT4	-	-	-	-	-	-
MXTWM	-	-	-	-	-	-
MNTCM	81.360 **	-12.334 *	-1.6887 ***	-	994.4	0.4519
TAR	-537.820 *	96.848 *	25.9075 *	-0.0944 *	1005.4	0.4475
P	-	-	-	-	-	-
P1	12.261 ***	-	-1.7063 ***	-0.0002 *	1015.6	0.4415
P2	-	-	-	-	-	-
P3	12.295 ***	-	-1.6408 ***	-0.0011 **	1009.6	0.4445
P4	12.181 ***	-	-1.5798 ***	-0.0022 **	1001.3	0.4485
PWM	-	-	-	-	-	-
PDM	9.142 ***	0.737 *	-1.3696 ***	-0.0059 **	1006.7	0.4468
M	-	-	-	-	-	-
M1	-	-	-	-	-	-
M2	-	-	-	-	-	-
M3	-	-	-	-	-	-
M4	12.233 ***	-	-1.5876 ***	-0.0623 **	1008.3	0.4451
PET	-	-	-	-	-	-
PET1	15.108 ***	-0.749 *	-1.7925 ***	-	1013.5	0.4425
PET2	-	-	-	-	-	-
PET3	-	-	-	-	-	-
PET4	11.979 ***	-	-1.7983 ***	0.0013 *	1011.8	0.4433

\*\*\* $p < 0.001$ ; \*\* $p < 0.01$ ; \* $p < 0.05$

**Supplementary Table 4.15:** Climate-dependent MSDR models for *Quercus suber* fitted at the 97.5<sup>th</sup> quantile arranged by AIC

model	$\alpha_0$	$\alpha_1$	$\beta_0$	$\beta_1$	AIC	pseudo-R <sup>2</sup>
T	55.009 **	-7.508 *	-1.9023 ***	-	1337.2	0.4857
T1	-	-	-	-	-	-
T2	-	-	-	-	-	-
T3	101.496 **	-15.722 **	-1.8724 ***	-	1326.9	0.4896
T4	12.040 ***	-	6.6223 **	-0.0284 ***	1285.4	0.5047
MNT	-	-	-	-	-	-
MNT1	578.103 *	-100.247 *	-33.3097 **	0.1113 *	1326.3	0.4905
MNT2	557.855 ***	-96.901 ***	-32.6036 ***	0.1104 ***	1313.2	0.4954
MNT3	-	-	-	-	-	-
MNT4	12.231 ***	-	3.3563 *	-0.0178 ***	1318.1	0.4928
MXT	12.122 ***	-	4.2310 ***	-0.0206 ***	1301.1	0.4991
MXT1	473.409 *	-81.306 *	-25.7606 *	0.0823 *	1336.4	0.4868
MXT2	12.247 ***	-	3.0873 *	-0.0171 ***	1317.3	0.4931
MXT3	12.343 ***	-	9.4775 **	-0.0384 ***	1243.8	0.5195
MXT4	-670.091 **	119.608 **	43.6583 ***	-0.1515 ***	1239.5	0.5217
MXTWM	12.097 ***	-	9.7879 ***	-0.0385 ***	1235.9	0.5223
MNTCM	511.050 **	-88.657 **	-30.2000 ***	0.1022 ***	1302.8	0.4992
TAR	12.922 ***	-	2.2551 **	-0.0144 ***	1248.3	0.5179
P	24.550 ***	-1.802 *	-2.7602 ***	0.0011 **	1254.7	0.5164
P1	-	-	-	-	-	-
P2	17.454 ***	-1.033 **	-2.4402 ***	0.0048 **	1283.4	0.5062
P3	-	-	-	-	-	-
P4	-	-	-	-	-	-
PWM	27.431 ***	-3.154 ***	-3.0211 ***	0.0096 ***	1310.9	0.4962
PDM	-	-	-	-	-	-
M	13.048 ***	-	-2.2457 ***	0.0061 ***	1264.9	0.5121
M1	12.923 ***	0.347 ***	-2.1668 ***	-	1321.2	0.4917
M2	14.486 ***	-1.064 *	-2.4802 ***	0.1007 **	1295.3	0.5019
M3	-	-	-	-	-	-
M4	-	-	-	-	-	-
PET	11.606 ***	-	-1.1484 ***	-0.0005 ***	1269.5	0.5104
PET1	-	-	-	-	-	-
PET2	-	-	-	-	-	-
PET3	11.948 ***	-	-1.2349 ***	-0.0043 ***	1233.6	0.5231
PET4	11.846 ***	-	-1.3656 ***	-0.0025 ***	1239.2	0.5211

\*\*\* $p < 0.001$ ; \*\* $p < 0.01$ ; \* $p < 0.05$

**Supplementary Table 5:** Functional traits and climatic requirements for the 15 species studied

Functional group	Species	ST	T (°C)	MTWM (°C)	MTCM (°C)	DT	P (mm)	RSP (mm)
<i>Coniferous</i>	<i>Pinus canariensis</i>	1	13-17	18-25	7-14	Very tolerant	400-1000	No limit
	<i>Pinus halepensis</i>	1.35	12-16	21-26	3-8	4.97 (0.03)	300-700	20-132
	<i>Pinus nigra</i>	2.1 (0.43)	9-12	20-23	1-4	4.38 (0.47)	600-1200	60-130
	<i>Pinus pinaster</i>	1.89 (0.21)	12-16	18-27	1-7	3	400-1600	70-150
	<i>Pinus pinea</i>	1	11-18	21-16	3-11	High	430-800	15-125
	<i>Pinus radiata</i>	2.97 (0.03)	10-13	16-20	4-8	3	1000-2000	100-290
	<i>Pinus sylvestris</i>	1.67 (0.33)	6-12	15-20	0-3	4.34 (0.47)	600-1200	> 100
	<i>Pinus uncinata</i>	1.2	4	< 15	< 0	3.88	> 800	> 200
<i>Broadleaf</i>	<i>Fagus sylvatica</i>	4.56 (0.11)	7.3-10	18	0	2.4 (0.43)	600-900	150-200
	<i>Quercus faginea</i>	-	8-16	15-26	(-3)-5	-	350-1400	> 100
	<i>Quercus ilex</i>	3.02 (0.19)	10-18	14-28	(-3)-11	4.72	> 450	75-100
	<i>Quercus petraea</i>	2.73 (0.27)	5-15	15-25	(-3)-7	3.02 (0.15)	600	150
	<i>Quercus pyrenaica</i>	2.55 (0.11)	11-16	12-22	(-5)-7	4.29 (0.21)	600	> 125
	<i>Quercus robur</i>	2.45 (0.28)	10	14-25	-10	2.95 (0.31)	600	200
	<i>Quercus suber</i>	-	13-16	20-26	4-5	-	> 500	23-165

Note: ST - Shade Tolerance, T - Mean Annual Temperature (°C), MTWM - Mean Temperature of the Warmest Month (°C), MTCM - Mean Temperature of the Coldest Month (°C), P - Mean Annual Precipitation (mm), and RSP - Required Summer Precipitation (mm). Data obtained from Niinemets and Valladares (2006) and Serrada et al. (2008). Shade tolerance is ranked as proposed by Baker (1949): 1 = Very intolerant, 2 = intolerant, 3 = moderately tolerant, 4 = tolerant, 5 = very tolerant.